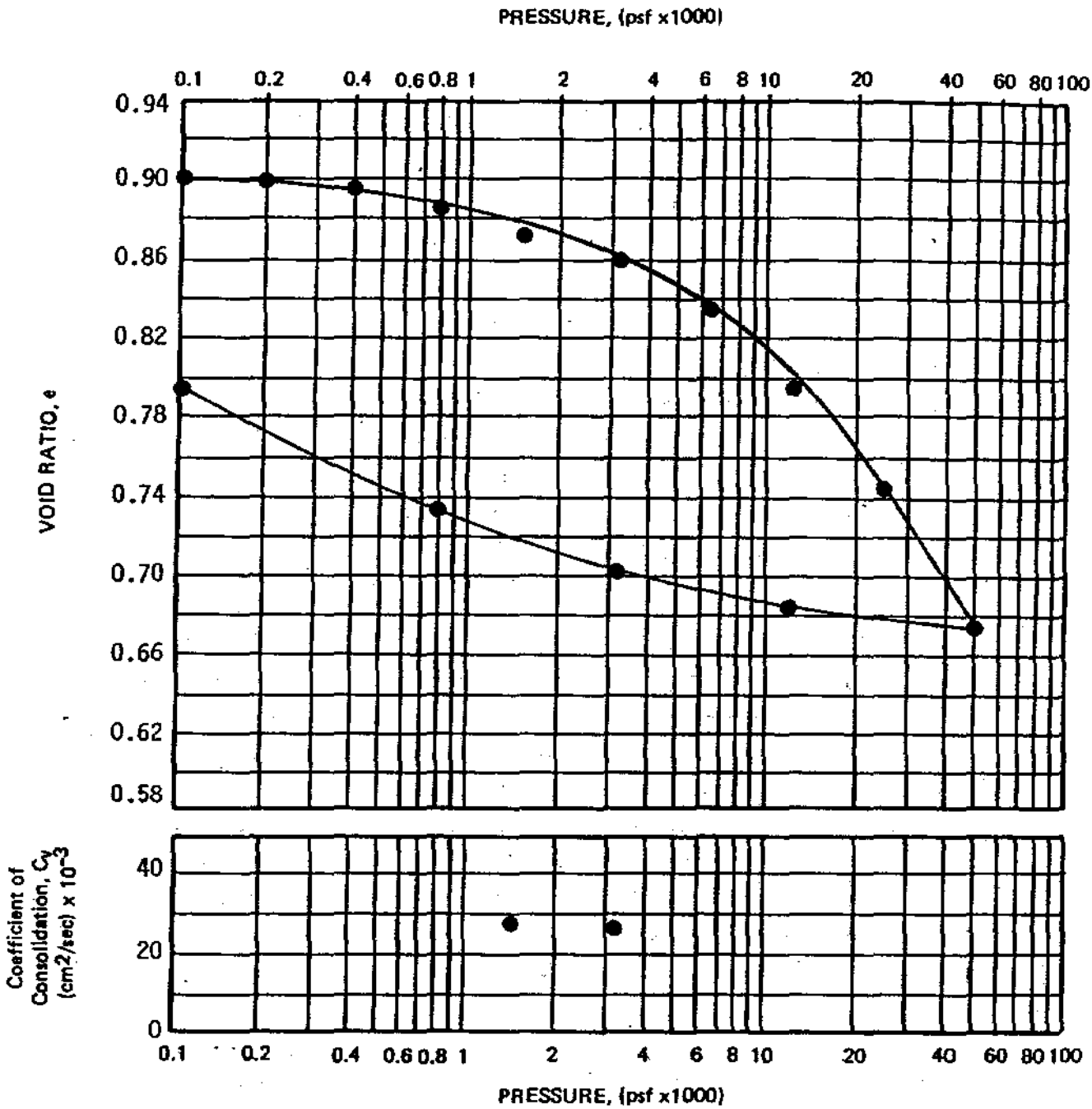

TYPE OF SPECIMEN Undisturbed (trimmed)			BEFORE TEST			AFTER TEST	
DIAMETER(in) 2.43	HEIGHT(in.) 0.80		MOISTURE CONTENT	w_o	33.1 %	w_f	29.7 %
OVERBURDEN PRESS., σ'_{vo}	350 psf		VOID RATIO	e_o	0.911	e_f	0.796
PRECONSOL PRESS.,(σ'_{vo}) max	-- psf		SATURATION	S_o	99 %	S_f	101 %
COMPRESSION INDEX,C_c	0.220		DRY DENSITY	γ_d	89 pcf	γ_d	94 pcf
LL 32	PL 26	PI 6		G_s	2.71		
CLASSIFICATION SILT (ML)		SOURCE Boring 14 at 6.3'					

Harding Lawson Associates
Engineers, Geologists & Geophysicists

Consolidation Test Report

Pt. Thomson Development Project
Winter 1982, Geotechnical Study
EXXON Company, U.S.A.

PLATE
D-137

DRAWN	JOB NUMBER	APPROVED	DATE	REVISED	DATE
JC	9612,031.08	DEB	4/82		

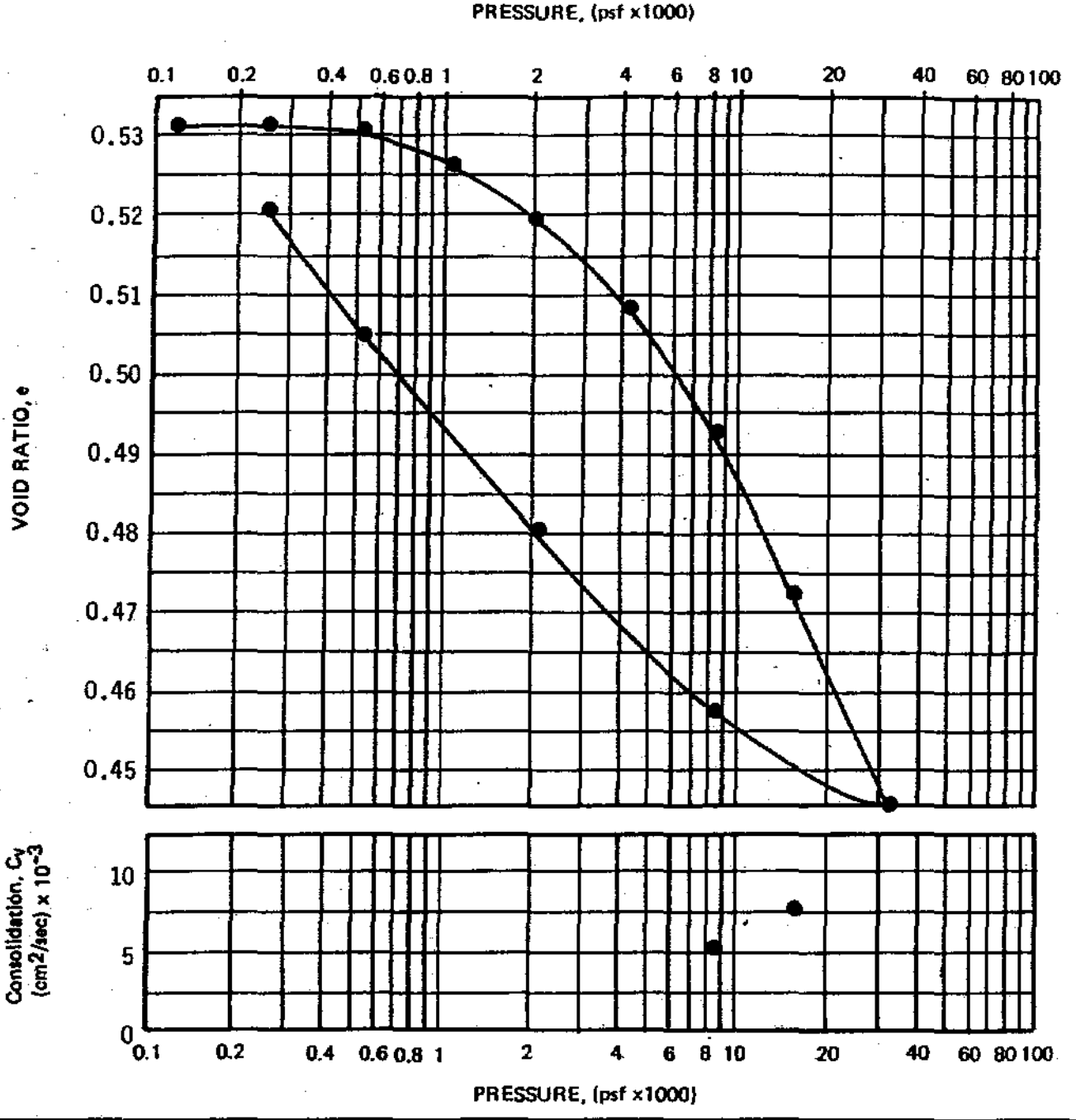

TYPE OF SPECIMEN Undisturbed(trimmed)		BEFORE TEST			AFTER TEST	
DIAMETER(in) 2.43	HEIGHT(in.) 0.80	MOISTURE CONTENT	w_o	19.5 %	w_f	19.1 %
OVERBURDEN PRESS., σ_{vo}' 920 psf		VOID RATIO	e_o	0.532	e_f	0.521
PRECONSOL PRESS.,(σ_{vo}') max psf		SATURATION	S_o	100 %	S_f	100 %
COMPRESSION INDEX, C_c 0.079		DRY DENSITY	γ_d	112 pcf	γ_d	119 pcf
LL 33	PL 19	PI 14		G_s 2.75		
CLASSIFICATION CLAY (CL)		SOURCE Boring 14 at 16.8'				

Harding Lawson Associates
Engineers, Geologists & Geophysicists

Consolidation Test Report

Pt. Thomson Development Project
Winter 1982, Geotechnical Study
EXXON Company, U.S.A.

PLATE **D-138**

DRAWN	JOB NUMBER	APPROVED	DATE	REVISED	DATE
JP	9612.031.08	DEB	4/82		

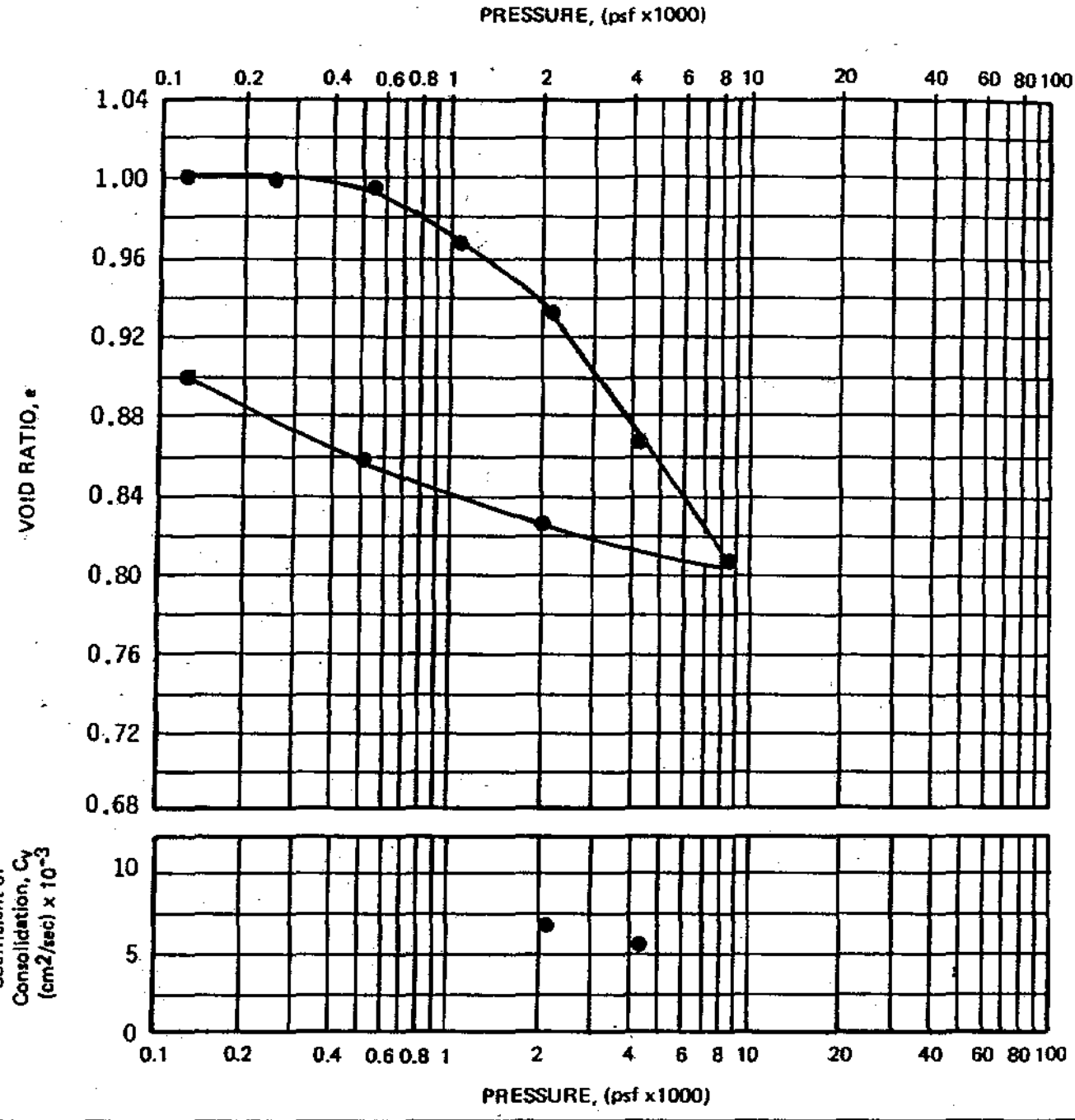

TYPE OF SPECIMEN Undisturbed(trimmed)			BEFORE TEST			AFTER TEST	
DIAMETER(in) 2.43	HEIGHT(in.) 0.80		MOISTURE CONTENT	w_o	40.5 %	w_f	34.8 %
OVERBURDEN PRESS., σ'_{vo} 290 psf			VOID RATIO	e_o	1.034	e_f	0.900
PRECONSOL PRESS.,(σ'_{vo}) max --- psf			SATURATION	S_o	100 %	S_f	102 %
COMPRESSION INDEX,C_c 0.204			DRY DENSITY	γ_d	81 pcf	γ_d	87 pcf
LL 46	PL 31	PI 5		G_s	2.65		
CLASSIFICATION SILT (ML)		SOURCE Boring 15 at 5.2'					

Harding Lawson Associates
Engineers, Geologists & Geophysicists

Consolidation Test Report
Pt. Thomson Development Project
Winter 1982, Geotechnical Study
EXXON Company, U.S.A.

PLATE
D-139

DRAWN	JOB NUMBER	APPROVED	DATE	REVISED	DATE
JP	9612,031.08	DEG	4/82		

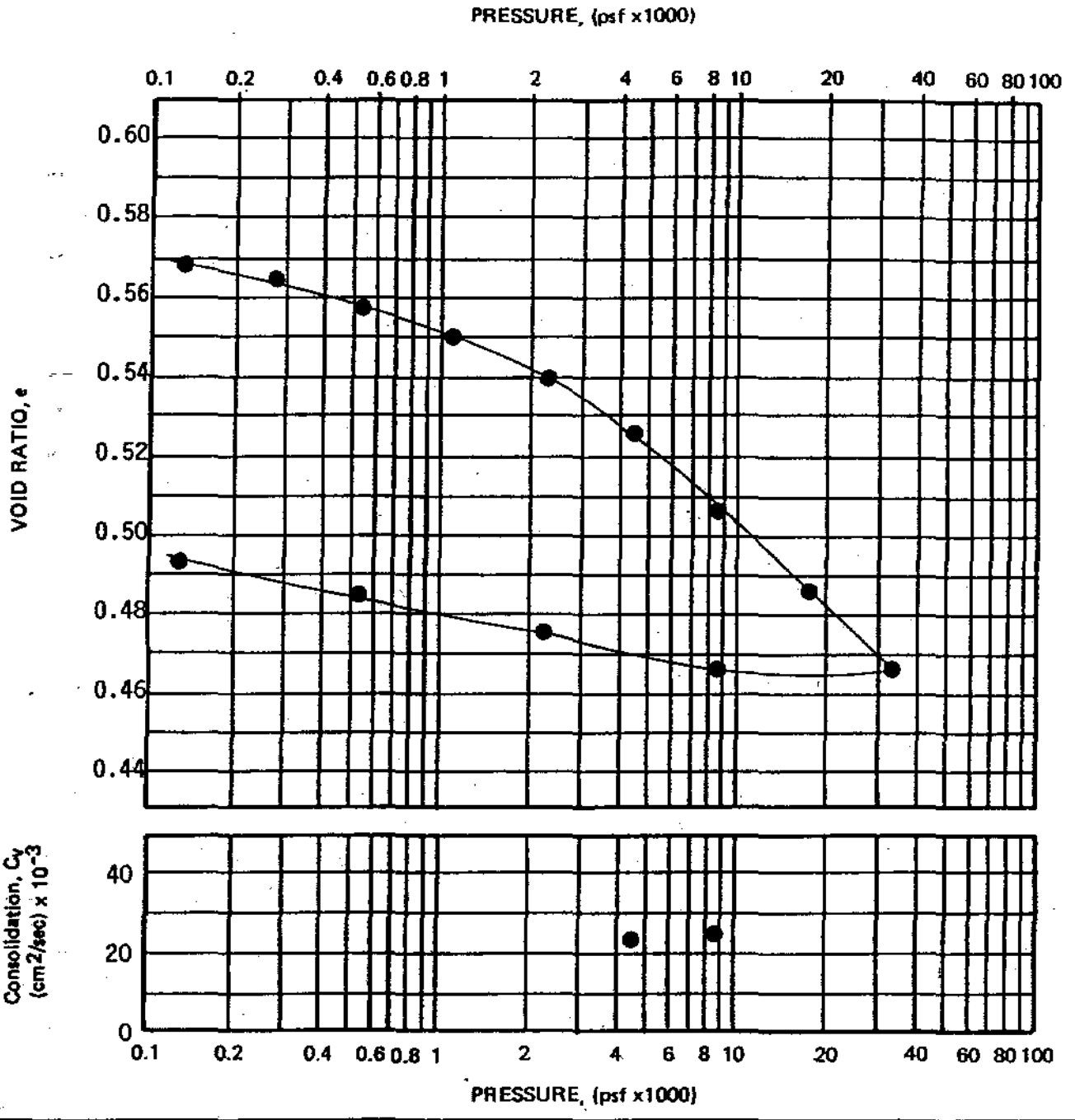

TYPE OF SPECIMEN Undisturbed(trimmed)			BEFORE TEST			AFTER TEST	
DIAMETER(in) 2.43	HEIGHT(in.) 0.80		MOISTURE CONTENT	w_o	21.5 %	w_f	18.6 %
OVERBURDEN PRESS., σ_{vo}'	1470 psf		VOID RATIO	e_o	0.586	e_f	0.492
PRECONSOL PRESS.,(σ_{vo}') max	-- psf		SATURATION	S_o	99 %	S_f	102 %
COMPRESSION INDEX,C_c	0.071		DRY DENSITY	γ_d	106 pcf	γ_d	113 pcf
LL --	PL --	PI --		G_s	2.69		
CLASSIFICATION SANDY SILT (ML)		SOURCE Boring 15 at 26.8'					

Harding Lawson Associates
Engineers, Geologists & Geophysicists

Consolidation Test Report

Pt. Thomson Development Project
Winter 1982, Geotechnical Study
EXXON Company, U.S.A.

PLATE **D-140**

DRAWN	JOB NUMBER	APPROVED	DATE	REVISED	DATE
VP	9612.031.08		4/82		

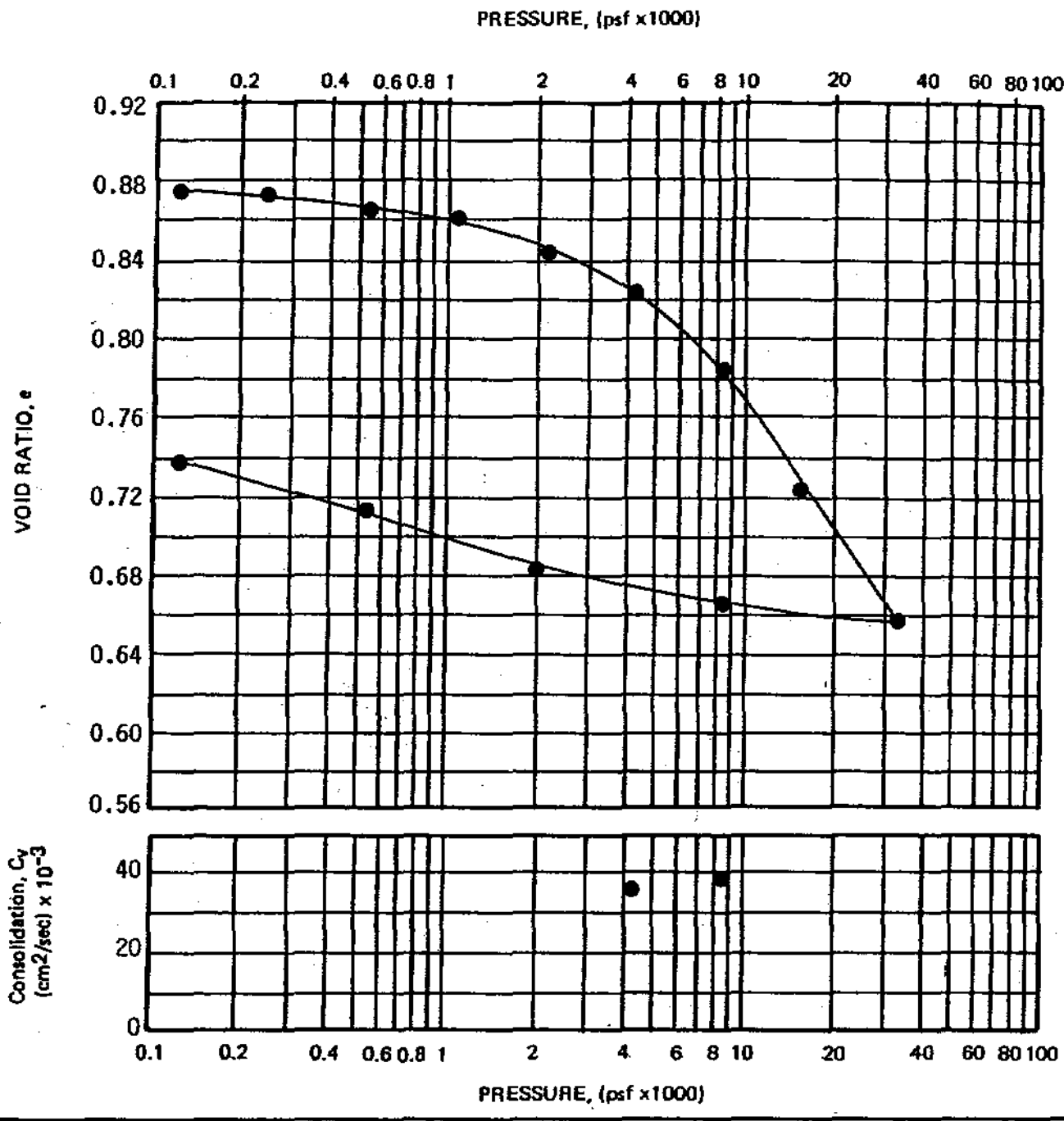

TYPE OF SPECIMEN Undisturbed (trimmed)		BEFORE TEST			AFTER TEST	
DIAMETER(in) 2.43	HEIGHT(in.) 0.80	MOISTURE CONTENT	w_o	32.6 %	w_f	26.8 %
OVERBURDEN PRESS., σ_{vo}'	190 psf	VOID RATIO	e_o	0.877	e_f	0.739
PRECONSOL PRESS.,(σ_{vo}') max	--- psf	SATURATION	S_o	100 %	S_f	103 %
COMPRESSION INDEX,C_c	0.208	DRY DENSITY	γ_d	90 pcf	γ_d	97 pcf
LL 25	PL 21	PI 4		G_s 2.71		
CLASSIFICATION CLAYEY SILT (CL-ML)		SOURCE Boring 17 at 3.5'				

Harding Lawson Associates
Engineers, Geologists & Geophysicists

Consolidation Test Report

Pt. Thomson Development Project
Winter 1982, Geotechnical Study
EXXON Company, U.S.A.

PLATE
D-141

DRAWN	JOB NUMBER	APPROVED	DATE	REVISED	DATE
JP	9612,031.08	DGB	4/82		

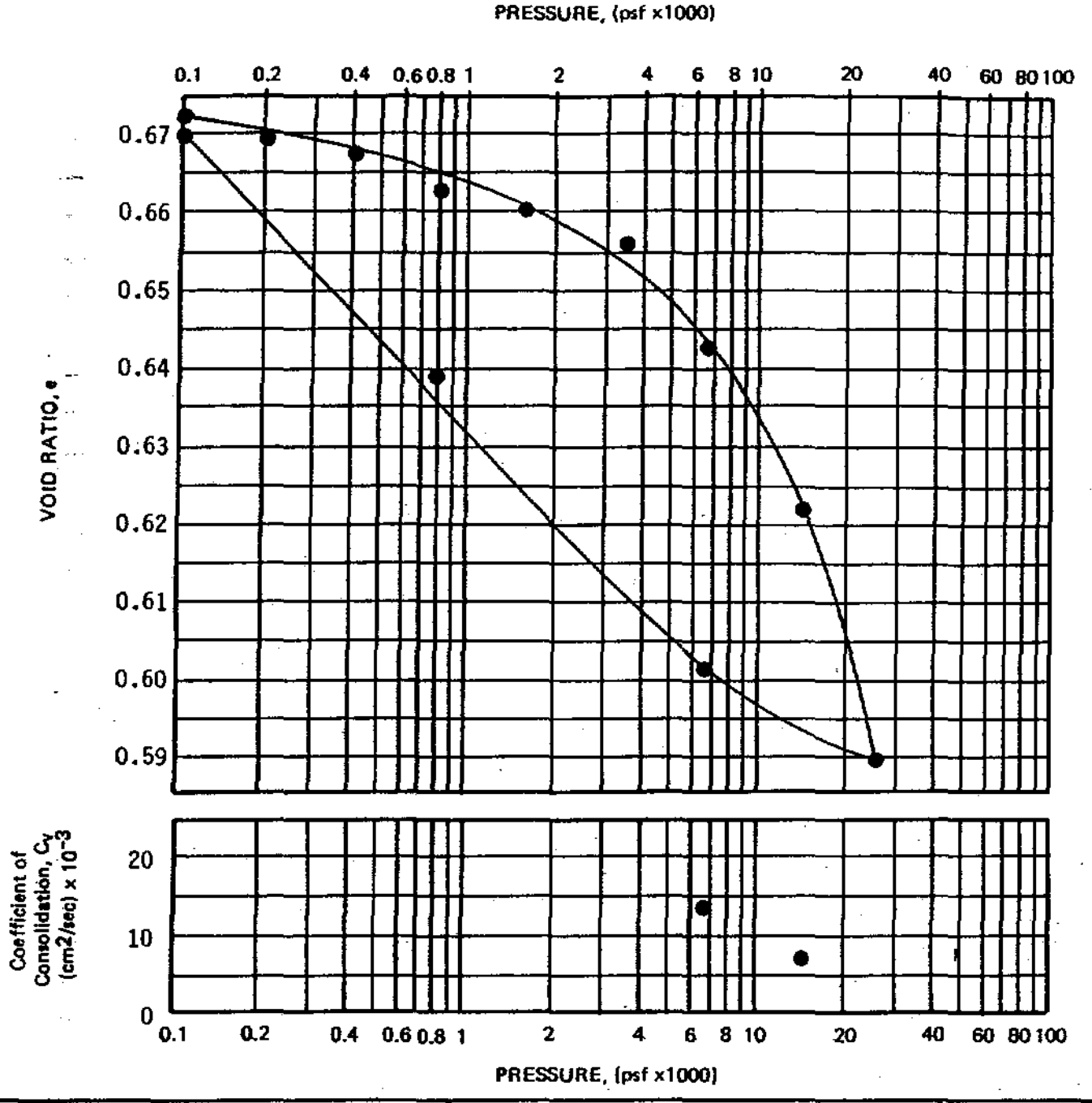

TYPE OF SPECIMEN Undisturbed (trimmed		BEFORE TEST				AFTER TEST	
DIAMETER(in) 2.43	HEIGHT(in.) 0.80	MOISTURE CONTENT	w_o	23.9 %	w_f	24.1 %	
OVERBURDEN PRESS., σ'_{vo}	1960 psf	VOID RATIO	e_o	0.678	e_f	0.670	
PRECONSOL PRESS.,(σ'_{vo}) max	-- psf	SATURATION	S_o	98 %	S_f	100 %	
COMPRESSION INDEX,C_c	0.084	DRY DENSITY	γ_d	103 pcf	γ_d	104 pcf	
LL --	PL --	PI --		G_s 2.78			
CLASSIFICATION CLAY (CL)		SOURCE Boring 17 at 35.7'					

Harding Lawson Associates
Engineers, Geologists & Geophysicists

Consolidation Test Report

Pt. Thomson Development Project
Winter 1982, Geotechnical Study
EXXON Company, U.S.A.

PLATE **D-142**

DRAWN	JOB NUMBER	APPROVED	DATE	REVISED	DATE
SP	9612,031.08	DEB	4/82		

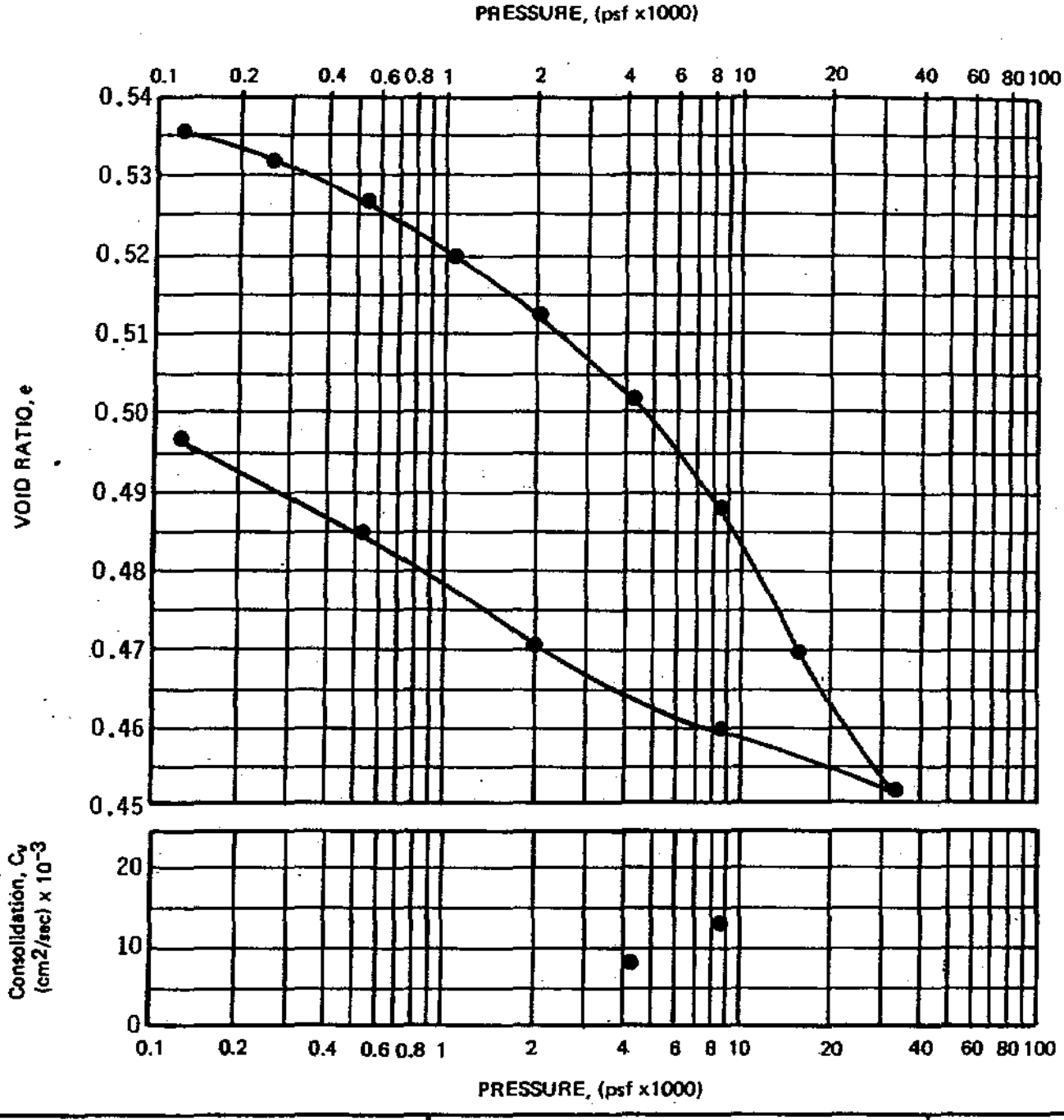

TYPE OF SPECIMEN Undisturbed(trimmed)		BEFORE TEST			AFTER TEST		
DIAMETER(in) 2.43	HEIGHT(in.) 0.80	MOISTURE CONTENT	w_o	20.1 %	w_f	17.9 %	
OVERBURDEN PRESS., σ'_{vo} 180 psf		VOID RATIO	e_o	0.552	e_f	0.497	
PRECONSOL PRESS.,(σ'_{vo}) max --- psf		SATURATION	S_o	100 %	S_f	100 %	
COMPRESSION INDEX,C_c 0.061		DRY DENSITY	γ_d	111 pcf	γ_d	115 pcf	
LL 26	PL 19	PI 7	G_s 2.76				
CLASSIFICATION CLAY (CL)		SOURCE Boring 21 at 3.3'					

Harding Lawson Associates
Engineers, Geologists & Geophysicists

Consolidation Test Report

Pt. Thomson Development Project
Winter 1982, Geotechnical Study
EXXON Company, U.S.A.

PLATE **D-143**

DRAWN	JOB NUMBER	APPROVED	DATE	REVISED	DATE
VP	9612,031.08	DB	4/82		

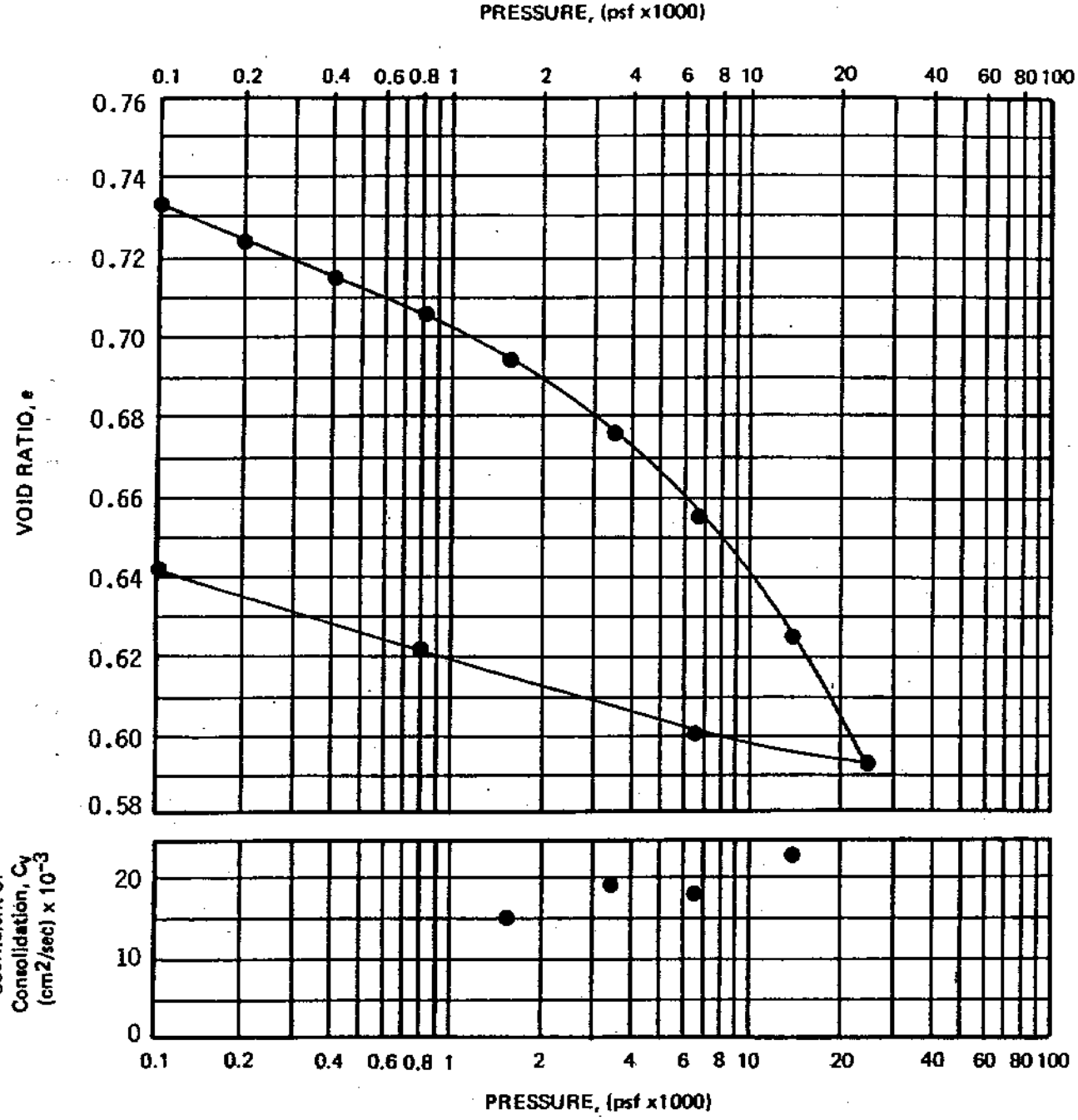

TYPE OF SPECIMEN Undisturbed (trimmed)		BEFORE TEST			AFTER TEST	
DIAMETER(in) 2.43	HEIGHT(in.) 0.80	MOISTURE CONTENT	w_o	27.0 %	w_f	22.8 %
OVERBURDEN PRESS., σ_{vo}'	1530 psf	VOID RATIO	e_o	0.758	e_f	0.641
PRECONSOL PRESS.,(σ_{vo}') max	-- psf	SATURATION	S_o	100 %	S_f	100 %
COMPRESSION INDEX,C_c	0.110	DRY DENSITY	γ_d	100 pcf	γ_d	107 pcf

LL --	PL --	PI --	G_s 2.81
CLASSIFICATION SANDY SILT (ML)		SOURCE Boring 21 at 27.8'	

Harding Lawson Associates
Engineers, Geologists & Geophysicists

Consolidation Test Report
Pt. Thomson Development Project
Winter 1982, Geotechnical Study
EXXON Company, U.S.A.

PLATE D-144

DRAWN	JOB NUMBER	APPROVED	DATE	REVISED	DATE
VF	9612.031.08	DFW	4/82		

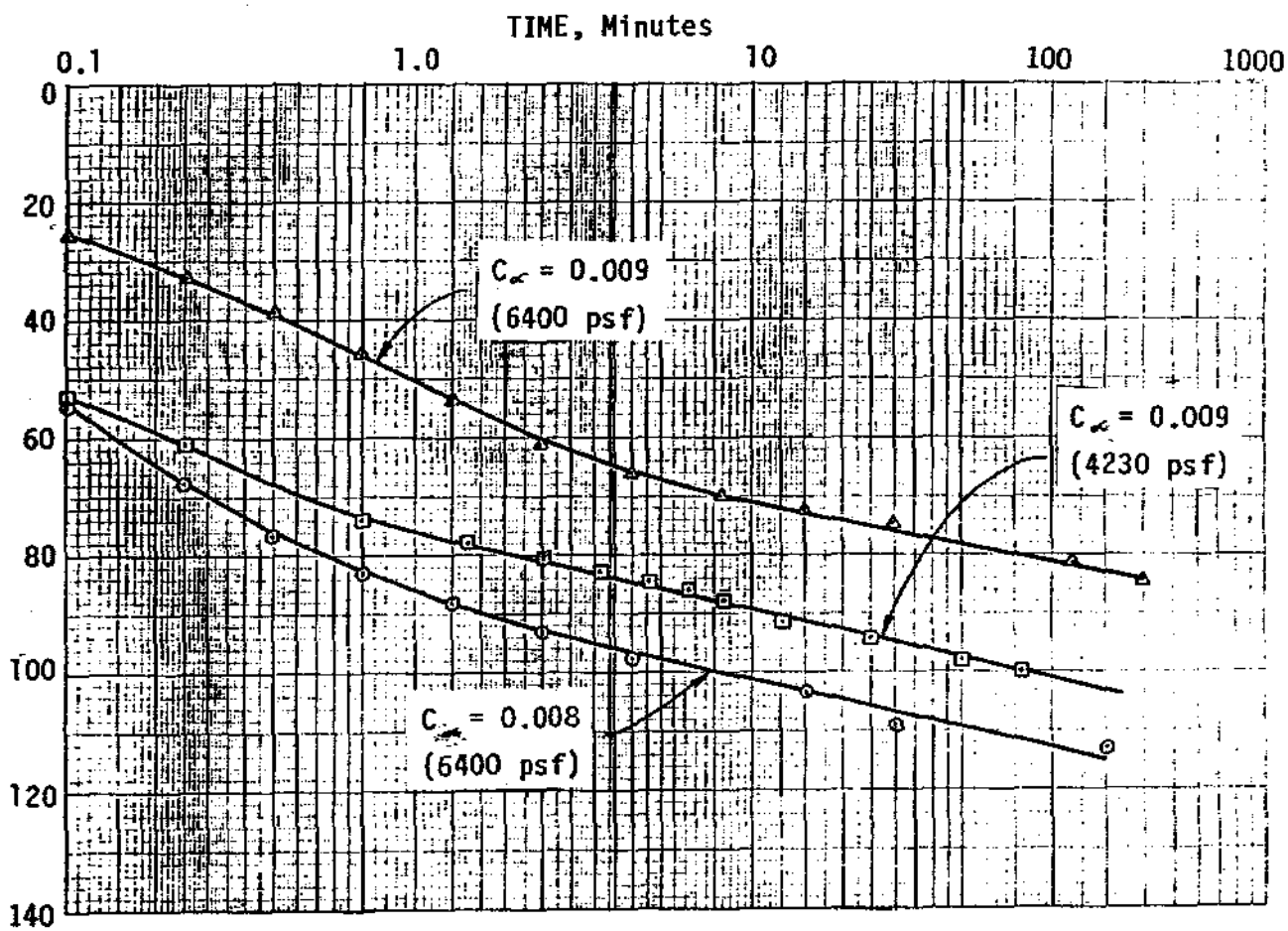

$$C_\alpha = \frac{\Delta H/H_0}{\log(t_2/t_1)}$$

Legend

- ⊡ SILTY SAND (SM), Boring 4 at 3.0'
- △ CLAY (CL), Boring 17 at 35.7'
- ⊙ SILT (ML), Boring 21 at 27.8'

Harding Lawson Associates
Engineers, Geologists
& Geophysicists

Coefficients of Secondary Consolidation PLATE

Pt. Thomson Development Project
Winter 1982, Geotechnical Study
EXXON Company, U.S.A.

D-145

DRAWN	JOB NUMBER	APPROVED	DATE	REVISED	DATE
	9612.031.08	DEB	4/82		

G. Thaw Consolidation Testing of Bonded Soil

Uniaxial thaw consolidation tests were performed on 28 undisturbed samples of bonded permafrost in accordance with the procedures developed by HLA. The testing device was a specially developed consolidometer that was designed to satisfy the necessary stress and thermal boundary conditions during one-dimensional thaw consolidation. The apparatus consists of a rigid, steel, thick-wall cyclinder, with porous stones at the top and bottom to allow the sample to drain. A vertical load is applied to the sample using a loading hanger which bears on a load cap assembly.

The samples were prepared in our cold room at a temperature of about $-8^{o}C$. Each sample was extruded from a 6-inch long brass liner having an inside diameter of 2.43-inches and approximately 1 inch of the soil was removed for electric conductivity tests. Next, the sample was trimmed to a length that varied between 4.5 and 5 inches, and the ends of the samples were cut flat. The sample was then inserted into the testing cyclinder, and the unit was transported from the cold room to the testing room. It was then mounted into the consolidation apparatus, and the sample was loaded to 500 psf and allowed to thaw at a room temperature of approximately $20^{o}C$. The load was then increased to 100 psf and the deformation recorded.

The results of the thaw consolidation tests are summarized on Plate D-146. In addition to a description of the sample, this plate contains information on the frozen state properties and the uniaxial thaw-strain. Data for thaw consolidation tests which were carried out to 58,000 psf load are presented on Plates D-147 through D-149.

Boring No.	Depth (ft)	USCS	Frozen Phase				Thawed Phase			
			Dry Density (pcf)	Ice Content (%)	Void Ratio	Saturation (%)	Dry Density (%)	Void Ratio	Thaw Load (psf)	Thaw Strain (%)
1	2.7	OL,Vx/Vr	15	301	10	78	39	3.0	1000	62
1	4.2	ML,Vx/Vr	47	92.6	2.60	97	105	0.610	1000	55
5	45.7	CL,Vr	86	33.6	0.977	93	88	0.934	1000	2
5	46.0	CL,Vr	67	36.2	1.50	65	70	1.4	1000	5
7	0.5	OL,Vx/Vr	34	108	3.80	74	40	3.1	1000	15
7	2.0	OL,Vx/Vr	19	250	7.70	88	51	2.2	1000	63
10	31.0	CL,Vr	108	21.6	0.574	100	115	0.574	1000	7
12	0.5	OL,Vx/Vr	78	27.6	1.168	70	97	0.743	1000	20
12	9.1	SM,Vx	93	19.2	0.818	70	115	0.470	1000	20
13	0.3	OL,Vx/Vr	53	54.9	2.06	78	66	1.458	1000	20
13	3.0	SP-SM,Vx	82	21.0	1.06	59	115	0.470	1000	29
13	17.5	ML,Vx/Vr	52	76.1	2.30	98	91	0.859	1000	44
15	39.6	CL,Vx/Vr	102	23.5	0.649	98	114	0.457	1000	8
15	49.1	CL,Vx/Vr	92	27.7	0.838	98	102	0.658	1000	9
16	3.1	SM,Vc/Vs	79	48.9	1.141	100	87	0.944	1000	9
16	5.1	ML,Vc/Vs	73	42.6	1.316	96	99	0.724	1000	26
16	9.1	SM,Vc/Vs	93	28.5	0.818	100	96	0.762	1000	4
16	24.6	ML,Vr	98	25.5	0.726	100	100	0.691	1000	3
18	1.0	OL, bonded	55	55.2	1.950	80	60	1.818	1000	17
19	24.5	ML,Vr	108	21.6	1.03	98	114	0.787	1000	5
23	0.0	ML,Vx	55	42.9	2.075	61	72	1.368	1000	23
23	1.0	ML,Vx	107	23.2	0.580	100	120	0.409	1000	11
23	10.8	ML,Vx	54	64.6	2.132	90	81	1.088	1000	33
23	19.0	CL,Vr	83	31.9	1.037	91	94	0.799	1000	14
23	39.5	CL,Vr	89	27.7	0.900	91	97	0.743	1000	8

Harding Lawson Associates
Engineers, Geologists
& Geophysicists

Thaw Consolidation Test Summary

Pt. Thomson Development Project
Winter 1982, Geotechnical Study
EXXON Company, U.S.A.

PLATE
D-146

DRAWN	JOB NUMBER	APPROVED	DATE	REVISED	DATE
SP	9612,031.08	DMS	4/82		

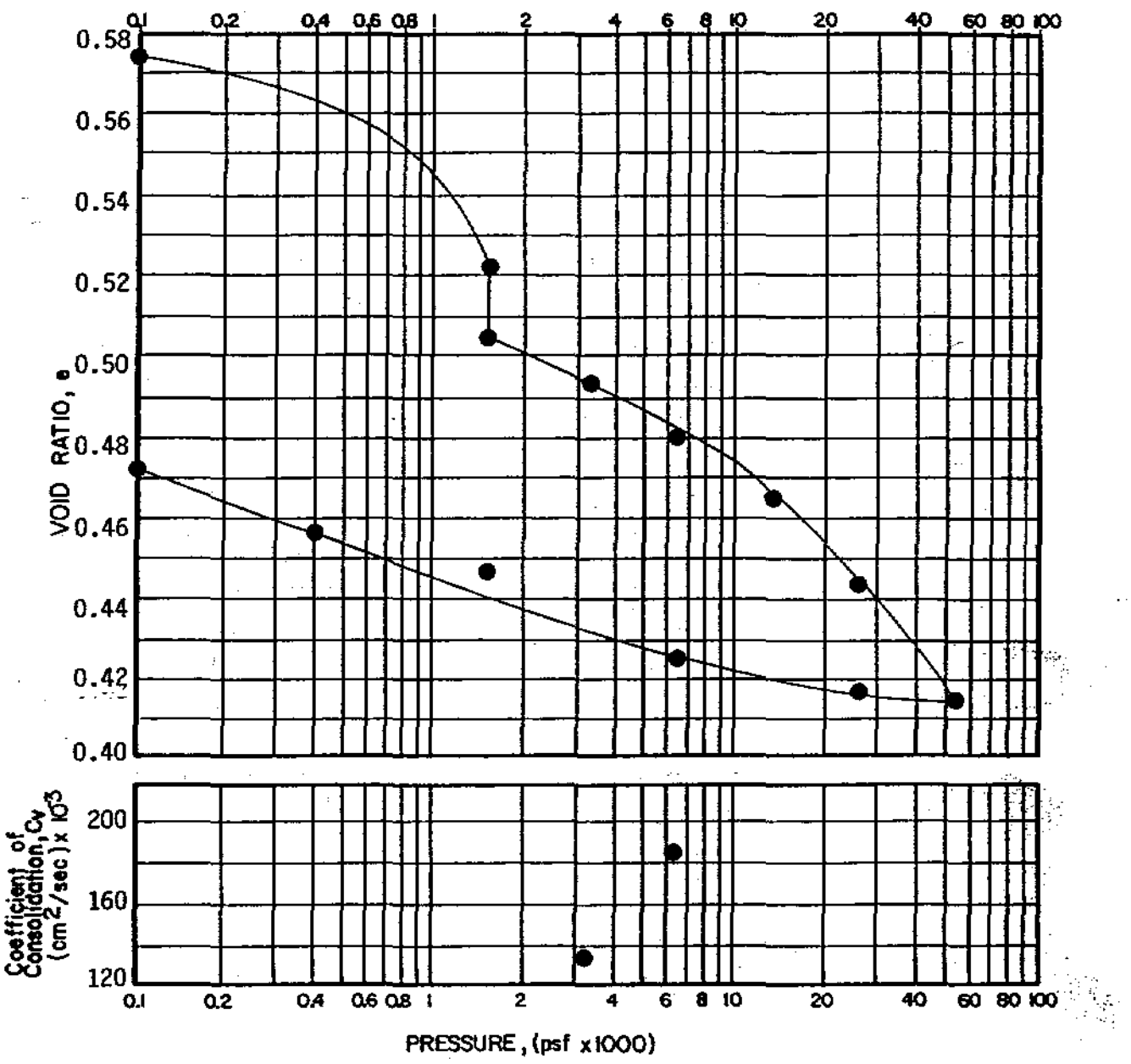

TYPE OF SPECIMEN Undisturbed (frozen)		BEFORE TEST			AFTER TEST	
DIAMETER(in) 2.43	HEIGHT(in) 1.80	MOISTURE CONTENT	w_o	21.6 %	w_f	17.5 %
OVERBURDEN PRESS., σ_{vo}' 1700 psf		VOID RATIO	e_o	0.574	e_f	0.471
PRECONSOL PRESS., $(\sigma_{vo}')_{max}$ --- psf		SATURATION	S_o	100 %	S_f	100 %
COMPRESSION INDEX, C_c 0.092		DRY DENSITY	γ_d	108 pcf	γ_d	115 pcf

LL 27	PL 21	PI 6	G_s 2.70 (Assumed)
CLASSIFICATION SILTY CLAY (CL)		SOURCE Boring 10 at 31.0'	

Harding Lawson Associates
Engineers, Geologists & Geophysicists

Thaw Consolidation Test Report

PT. Thomson Development Project
Winter 1982, Geotechnical Study
EXXON Company, U.S.A.

PLATE **D-147**

DRAWN	JOB NUMBER	APPROVED	DATE	REVISED	DATE
JC	9612,031.08	DEB	4/82		

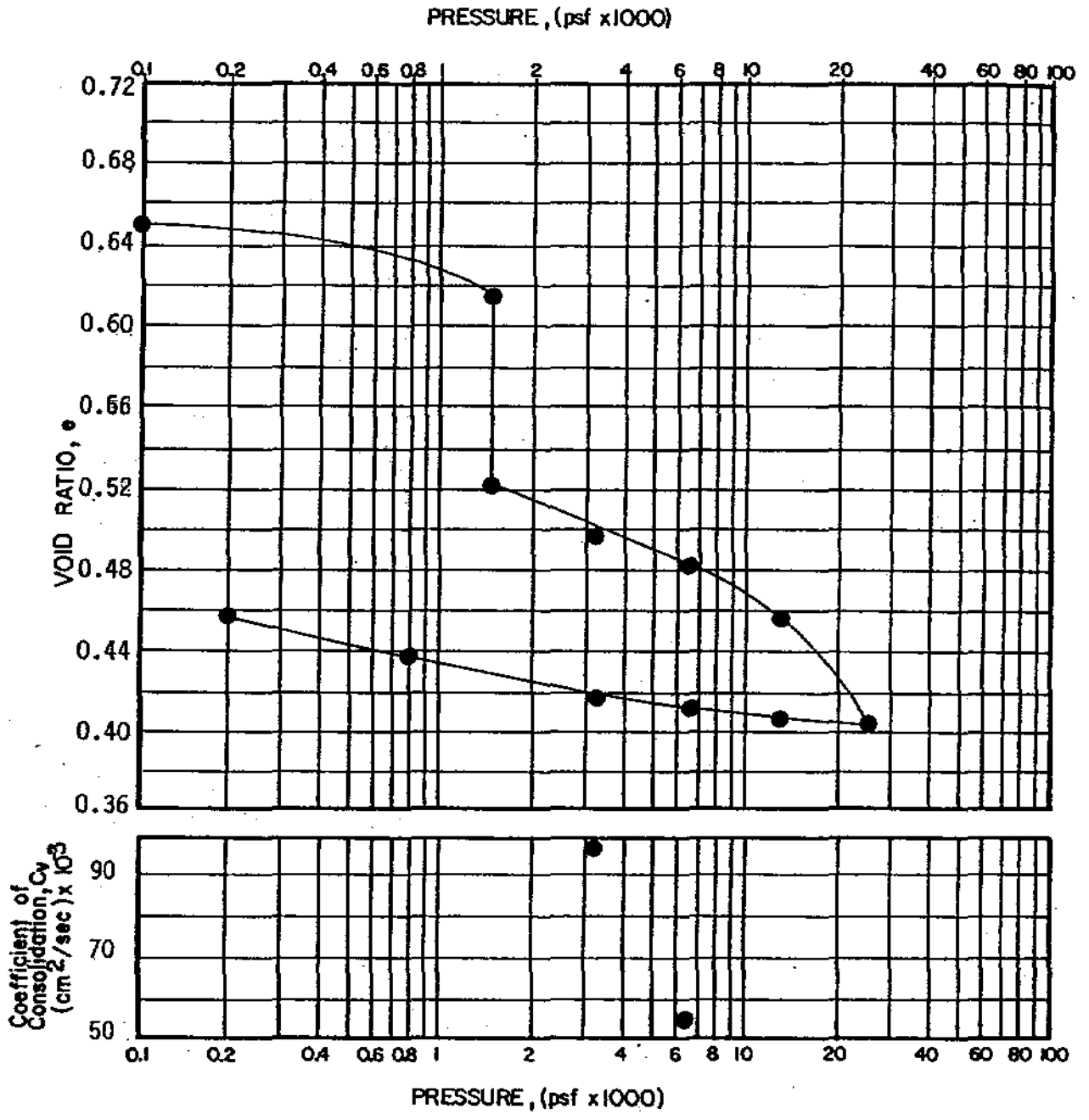

TYPE OF SPECIMEN Undisturbed (frozen)			BEFORE TEST (Frozen)			AFTER TEST	
DIAMETER(in) 2.43	HEIGHT(in) 1.80		MOISTURE CONTENT	w_o	23.5 %	w_f	17.0 %
OVERBURDEN PRESS, σ_{vo}'	2170	psf	VOID RATIO	e_o	0.649	e_f	0.457
PRECONSOL PRESS., $(\sigma_{vo}')_{max}$	---	psf	SATURATION	S_o	98 %	S_f	100 %
COMPRESSION INDEX, C_c	0.230		DRY DENSITY	γ_d	102 pcf	γ_d	114 pcf
LL 28	PL 21		PI 7		G_s 2.70 (Assumed)		
CLASSIFICATION SILTY CLAY (CL)			SOURCE Boring 15 at 39.5'				

Harding Lawson Associates
Engineers, Geologists
& Geophysicists

Thaw Consolidation Test Report

Pt. Thomson Development Project
Winter 1982, Geotechnical Study
EXXON Company, U.S.A.

PLATE **D-148**

DRAWN	JOB NUMBER	APPROVED	DATE	REVISED	DATE
	9612,031.08	DEB	4/82		

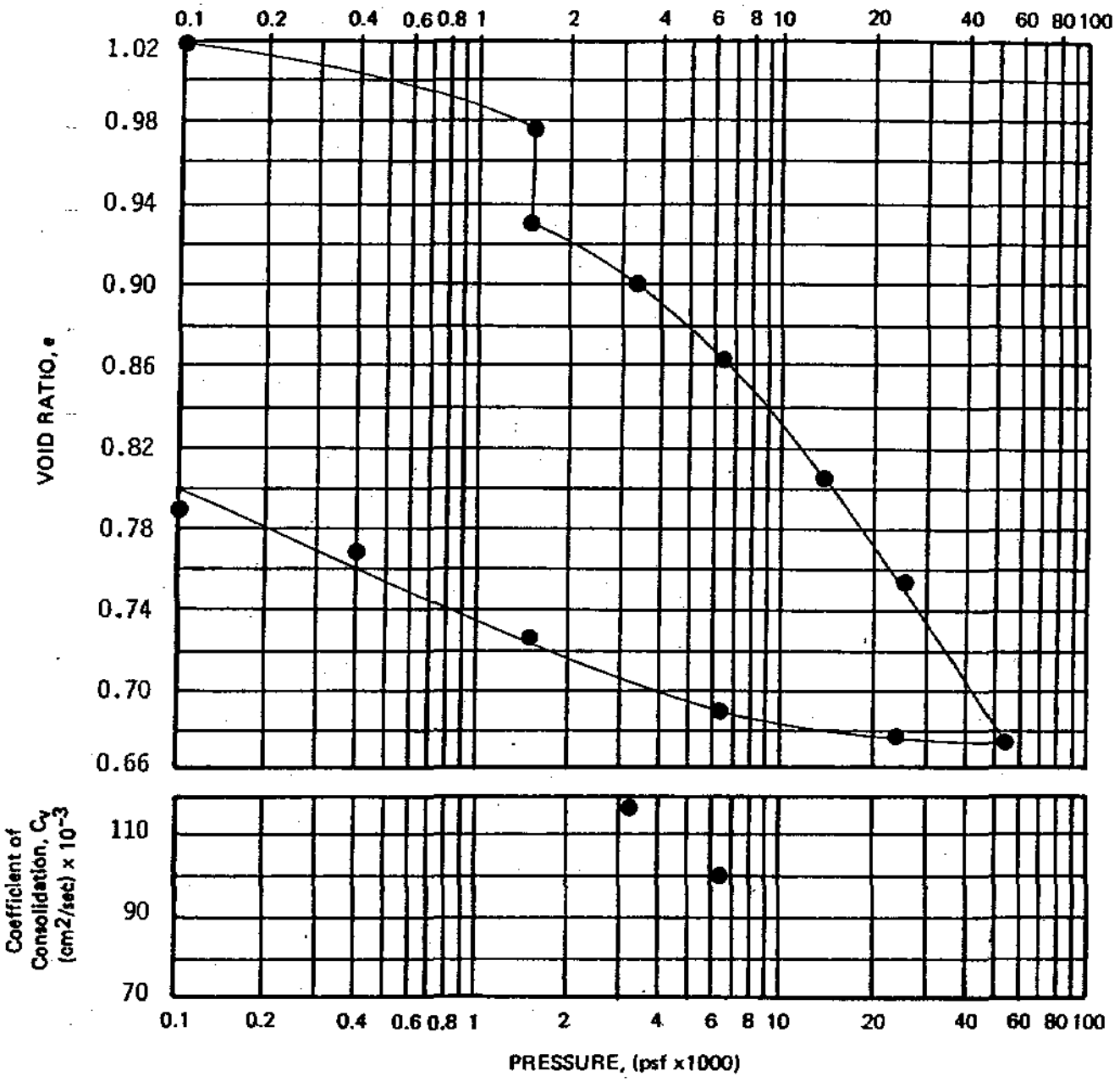

TYPE OF SPECIMEN Undisturbed (frozen)		BEFORE TEST (Frozen)			AFTER TEST		
DIAMETER(in) 2.43	HEIGHT(in.) 1.80	MOISTURE CONTENT	w_o	21.6 %	w_f	29.3 %	
OVERBURDEN PRESS., σ_{vo}'	1350 psf	VOID RATIO	e_o	1.025	e_f	0.787	
PRECONSOL PRESS.,(σ_{vo}') max	--- psf	SATURATION	S_o	98 %	S_f	100 %	
COMPRESSION INDEX,C_c	0.219	DRY DENSITY	γ_d	108 pcf	γ_d	114 pcf	
LL 38	PL 26	PI 12		G_s 2.70 (Assumed)			
CLASSIFICATION CLAYEY SILT (ML)		SOURCE Boring 19 at 24.5'					

Harding Lawson Associates
Engineers, Geologists & Geophysicists

Thaw Consolidation Test Report

Pt. Thomson Development Project
Winter 1982, Geotechnical Study
EXXON Company, U.S.A.

PLATE
D-149

DRAWN	JOB NUMBER	APPROVED	DATE	REVISED	DATE
VP	9612.031.08	DGB	4/82		

A general relationship for thaw consolidation was obtained by comparing the values of thaw strain and frozen dry density plotted on Plate IV-22 for fine-grained soil while data for gravels are presented on Plate V-8. The data for Plate V-8 are based on other studies. Because samples having a broad range of frozen dry densities were used, it was possible to establish a curve from which thaw consolidation could be estimated. The curve on Plate IV-22 represents the mean thaw strain plus one standard deviation and shows that when the frozen dry densities are greater than approximately 95 pcf, the thaw strains are less than 8 percent. As the frozen dry densities of the samples decrease, the scatter of thaw strain values becomes greater. The increase in thaw strain is approximately 0.7 percent per pcf decrease in dry density.

Literature on thaw consolidation is very limited, particularly for Beaufort Sea soils. The results of the thaw consolidation tests that were performed for this project can be compared with the results obtained for three other Beaufort Sea projects. These results are contained in the following reports: "Subsurface Soil Investigation, Duck Island Wild Cat, Beaufort Sea, Alaska" (R & M Consultants, 1978), "Geotechnical Investigation, Beaufort Sea, Alaska" (HLA/USGS, 1979) and "Duck Island Development Project, Beaufort Sea, Alaska" (HLA, 1981). The data are in agreement with the results of our tests for this project.

H. Thermal Conductivity

Measurements of radial thermal conductivity were made using the "thermal needle method." A detailed discussion of the theory and development of this method is presented by Mitchell and Kao (1978).

In simplified terms, thermal energy is applied at a known constant rate to a probe embedded in a sample. The temperature of the probe is measured as a function of time. By plotting the temperature change versus the log of time, a straight-line relationship is produced with a slope that is proportional to the thermal conductivity. The general equation used for calculating the thermal conductivity is:

$$K = \frac{Q\,[\ln \Delta t]}{4\pi\Delta T} \qquad \text{(D-3)}$$

Where: K = thermal conductivity (Btu/ft-hr-^{o}F)

Q = thermal energy input per unit length per unit time (Btu/ft-hr)

T = temperature change corresponding to time

t = time change corresponding to temperature

By substituting specific probe information, Equation D-3 yields the following:

$$K = \frac{CI^2 R\pi \ln (t_2/t_1)}{4\pi\,(T_2 - T_1)} \qquad \text{(D-4)}$$

Where: C = constant (1 watt/ft = 3.413 Btu/hr)

I^2 = current (amp)

R = probe unit resistance (4.503 ohm/ft)

By substitution:

$$K = \frac{1.223\, I^2 \ln (t_2/t_1)}{(T_2 - T_1)} \qquad \text{(D-5)}$$

The following equipment was used for the conductivity tests:

Thermal needle: The thermal needle consists of 1/8-inch O.D. stainless steel tube, Copper Constantan 0.003-inch-diameter thermocouple wire, Constantan #30 heat source wire, and #16 copper wire leads.

Heat source power supply: A Hewlett-Packard Model 6284A DC Power Supply, with constant voltage from 0 to 20 volts, and constant current from 0 to 3 amps, was used as the heat source.

Thermocouple signal amplifier: This device is our Omega "Omni-Amp IIB" with built-in ice point reference, that is capable of amplifying the thermocouple signal 100 times.

Recording equipment: An Omega single-channel strip chart recorder, Model 555 was used.

Most of the samples tested were unbonded soils. However, five bonded samples were tested as frozen samples. The testing procedure for these samples was as follows:

1. The bulk weight and sample dimensions were measured to determine soil density.

2. An 1/8-inch-diameter hole was drilled from top to bottom through the center of the sample, and the probe was inserted into the hole. Next, both ends were capped and the sample was immersed in a constant temperature bath, maintained at the specified initial temperature until the sample temperature was stabilized.

3. Power was applied to the Constantan line, and the change in temperature with time was recorded on the chart recorder. The input power generally varied from 0.400 to 0.450 amp for both the frozen and the thawed tests. The test was run for 10 minutes, after which the power was turned off. This procedure was repeated until consistent results were obtained at each temperature.

4. The temperature, expressed in millivolts, plotted against the log of time, and the slope of the straight line portion of this curve was determined. The radial thermal conductivity was then calculated using Equation D-5.

5. Finally, the moisture content was determined. Index property tests were also performed when necessary.

A summary of the thermal conductivity test results is presented on Plate D-150. The results of individual thermal conductivity tests, plots of millivolts versus log time, and any index tests that were performed on the sample are presented on Plates D-151 through D-163.

Two log cycles of data are produced when our test procedure is used. For this report, the first log cycle, which contains the time increment of 0.1 to 1 minute, was omitted because a nonlinear relationship was produced due to problems associated with the seating of the probe. This nonlinearity disappeared within 1 minute of applying the probe, and the thermal conductivity was determined from the straight line portion of the plot in the second log cycle. Two conductivity tests were made on each sample to ensure that the correct thermal conductivity was determined.

The variation of thermal conductivity with density is plotted for the tested samples on Plate IV-23 along with the data from the Duck Island Development project (HLA, 1981). On this plate, the two thermal conductivity values for each sample are connected by a line. It can be seen that the thermal conductivity increases with increases in dry density for both the thawed and frozen samples. Typically, the thermal conductivity will also increase with increases in moisture content. However, this was not observed in these tests, perhaps because of the small range of moisture contents tested.

In general, the thermal conductivity varies with the texture of the soil. At a given density and moisture content, the conductivity is relatively high in coarse-grained soils, such as sands and gravels, and lower in fine-grained soils, such as silts and clays. For the one thermal conductivity test that

Boring No.	Depth (ft)	USCS	Dry Density (pcf)	Moisture Content (%)			Thermal Conductivity Btu/Ft-hr-°F	
				LL	PL	Natural	Frozen*	Thawed
4	12.4	ML	78	---	---	38.8	---	1.09
5	19.2	CL	79	31	21	39.5	---	0.99
8	12.2	ML	103	---	---	22.6	---	1.38
9	0.5	SM	105	---	---	22.1	---	1.41
9	46.4	CL	93	---	---	29.3	---	1.30
12	0.0	OL, Vx/Vr	11	---	---	406	0.55	---
13	18.0	ML, Vx/Vr	29	34	25	154	1.20	---
14	31.1	ML	105	---	---	22.8	---	1.24
18	0.3	OL	31	---	---	149	1.07	---
21	16.1	ML	97	---	---	27.3	---	1.42
21	31.0	CL	101	---	---	24.4	---	1.49
23	0.5	ML, Vx	78	21	13	30.3	1.46	---
23	12.5	CL, Vr	70	33	22	43.9	1.17	---

* Test run at temperature of 15° F.

Harding Lawson Associates
Engineers, Geologists & Geophysicists

Thermal Conductivity Test Summary
Pt. Thomson Development Project
Winter 1982, Geotechnical Study
EXXON Company, U.S.A.

PLATE **D-150**

DRAWN	JOB NUMBER	APPROVED	DATE	REVISED	DATE
	9612,031.08		4/82		

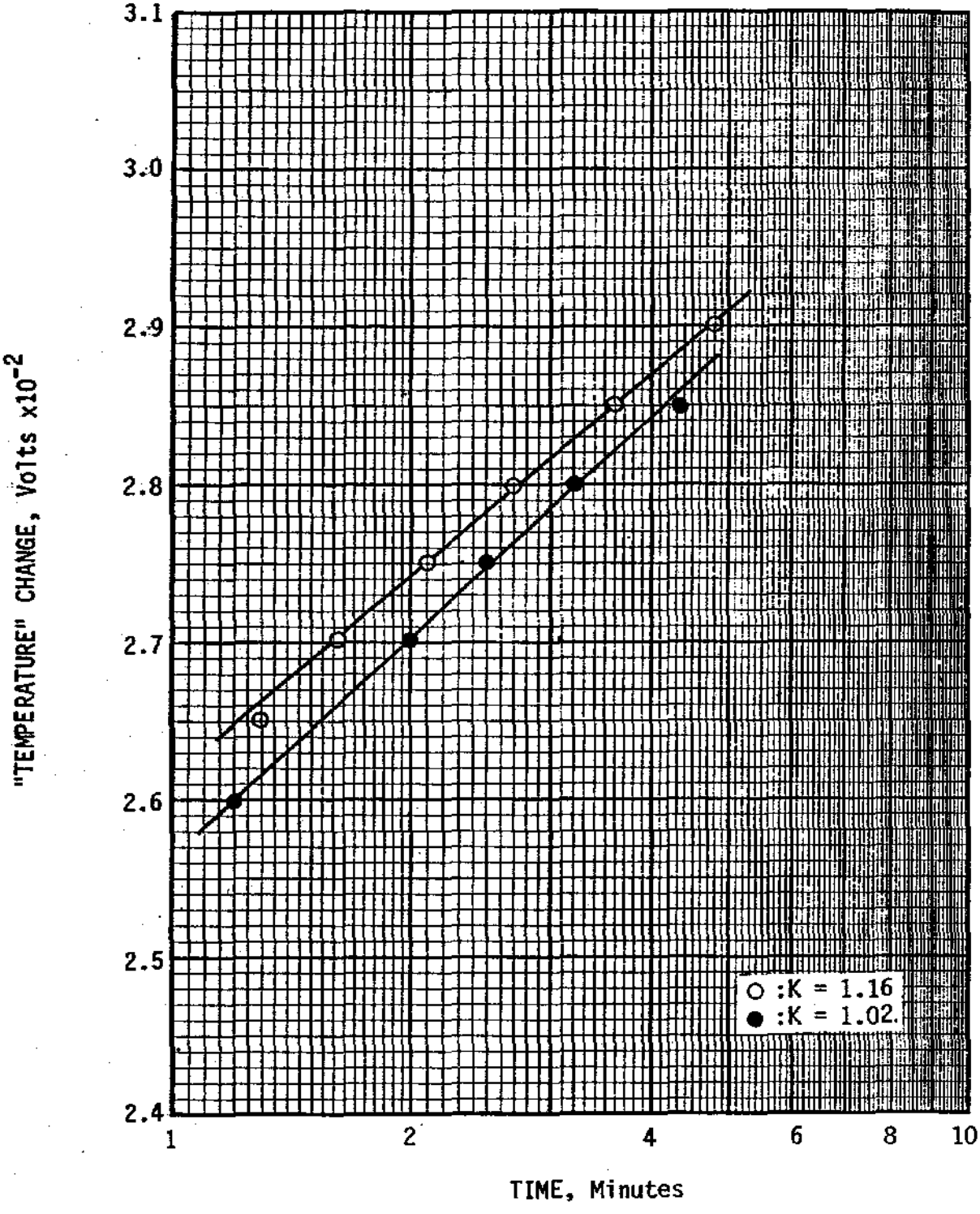

CLASSIFICATION SILT (ML)				**SOURCE** Boring 4 at 12.4'			
MOISTURE CONTENT 38.8 %		**DRY DENSITY** 78	pcf	□ FROZEN / ■ THAWED **THERMAL CONDUCTIVITY** 1.09		Btu / Ft-hr-°F	
LL 33 %	**PL** 26 %	**-200 sieve** 90.1	%	**ORGANIC CONTENT** ----		%	

Harding Lawson Associates
Engineers, Geologists & Geophysicists

Thermal Conductivity
Pt. Thomson Development Project
Winter 1982, Geotechnical Study
Exxon Company, U.S.A.

PLATE **D-151**

DRAWN	JOB NUMBER	APPROVED	DATE	REVISED	DATE
	9612,031.08	DAB	4/82		

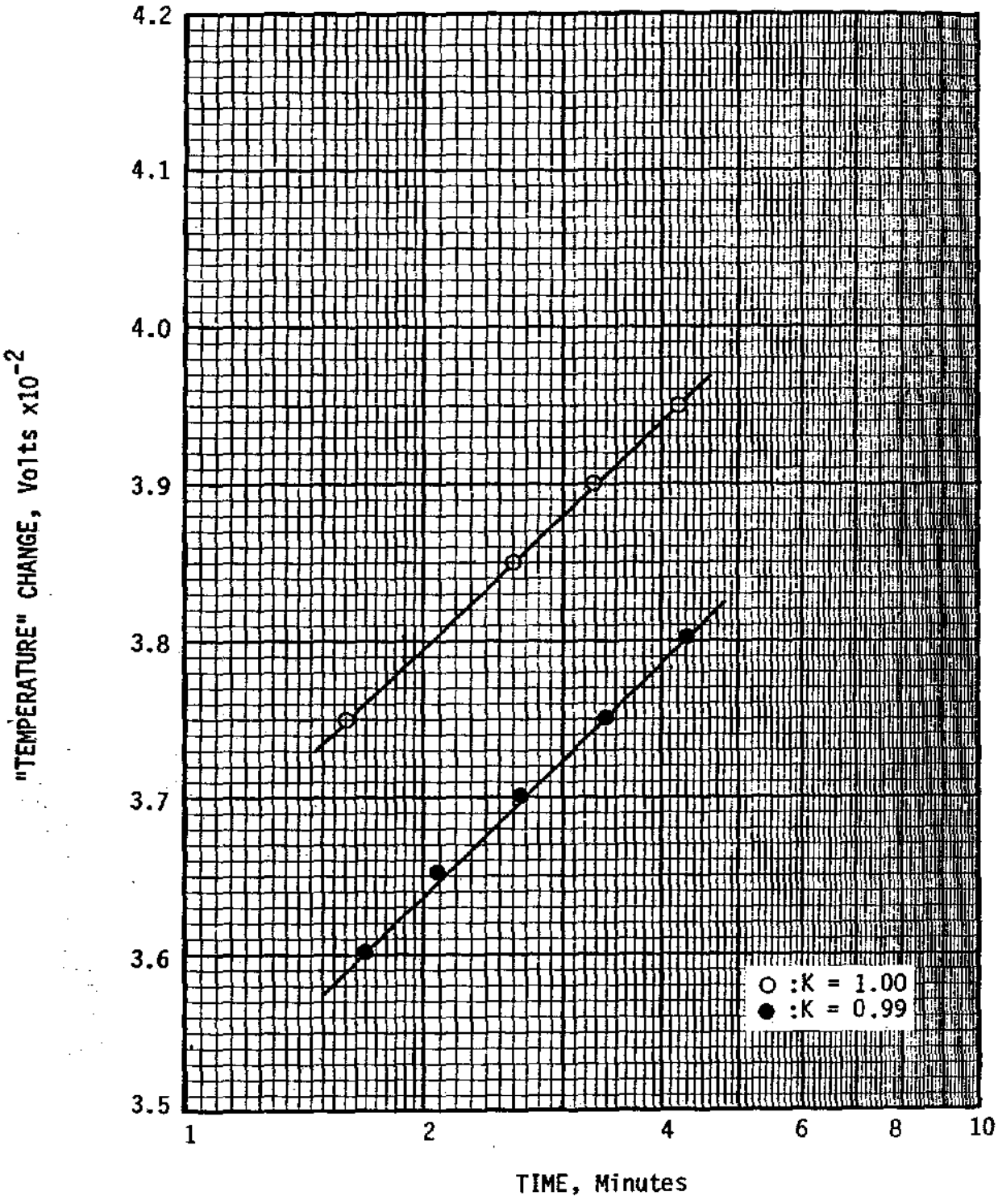

CLASSIFICATION	SILTY CLAY (CL)				**SOURCE**	Boring 5 at 19.2'	
MOISTURE CONTENT	39.5 %	**DRY DENSITY**	79	pcf	☐ FROZEN / ■ THAWED **THERMAL CONDUCTIVITY**	0.99	Btu / Ft-hr-°F
LL	31 %	**PL**	21 %	**-200 sieve**	--- %	**ORGANIC CONTENT**	---- %

Harding Lawson Associates
Engineers, Geologists & Geophysicists

Thermal Conductivity

Pt. Thomson Development Project
Winter 1982, Geotechnical Study
Exxon Company, U.S.A.

PLATE **D-152**

DRAWN	JOB NUMBER	APPROVED	DATE	REVISED	DATE
	9612,031.08		4/82		

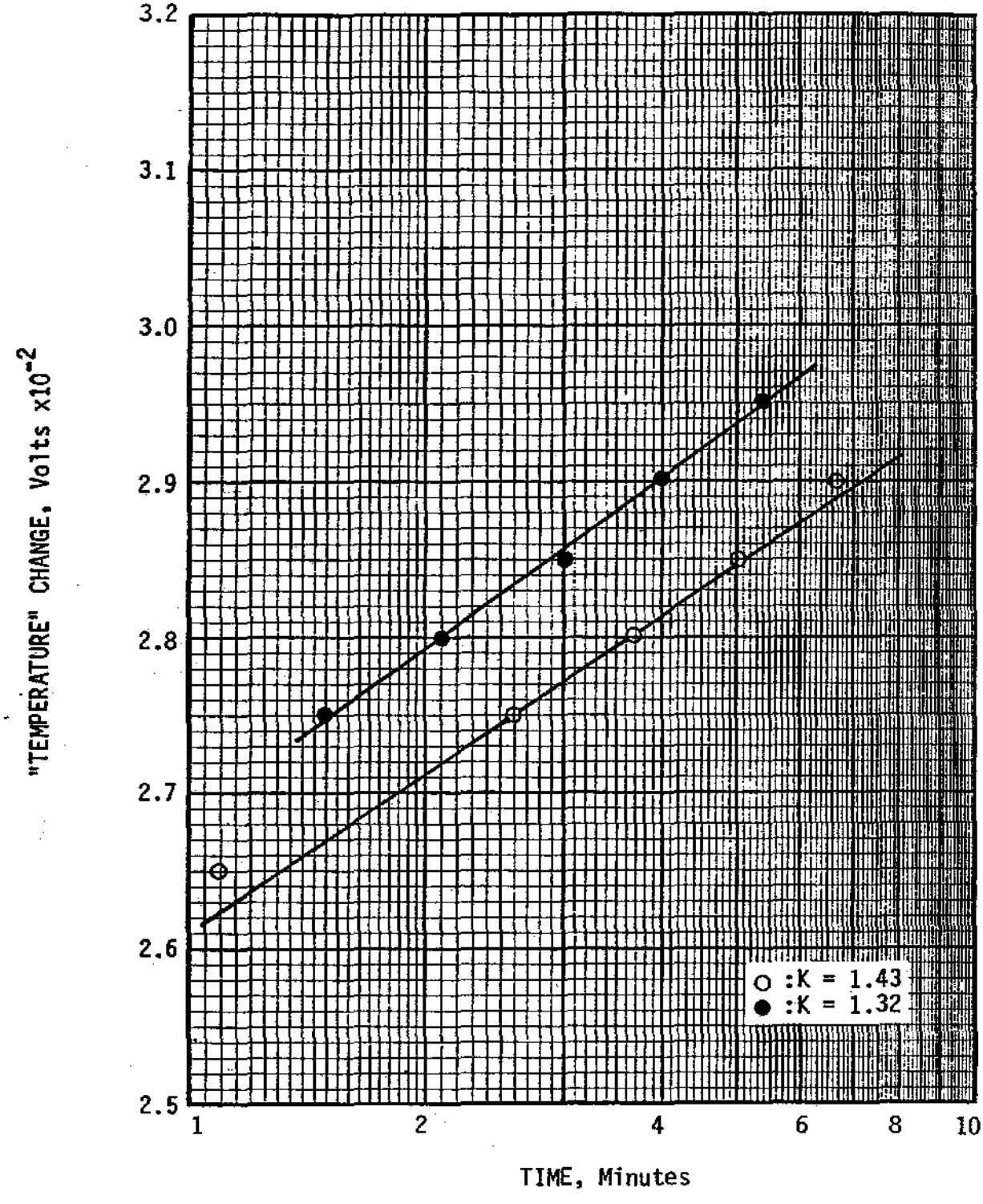

CLASSIFICATION SILT (ML)			**SOURCE** Boring 8 at 12.2'
MOISTURE CONTENT 22.6%	**DRY DENSITY** 103 pcf	□ FROZEN / ■ THAWED **THERMAL CONDUCTIVITY** 1.38	Btu / Ft-hr-°F
LL -- %	**PL** -- %	**-200 sieve** --- %	**ORGANIC CONTENT** ----- %

Harding Lawson Associates
Engineers, Geologists
& Geophysicists

Thermal Conductivity

Pt. Thomson Development Project
Winter 1982, Geotechnical Study
Exxon Company, U.S.A.

PLATE **D-153**

DRAWN	JOB NUMBER	APPROVED	DATE	REVISED	DATE
JP	9612,031.08	DEB	4/82		

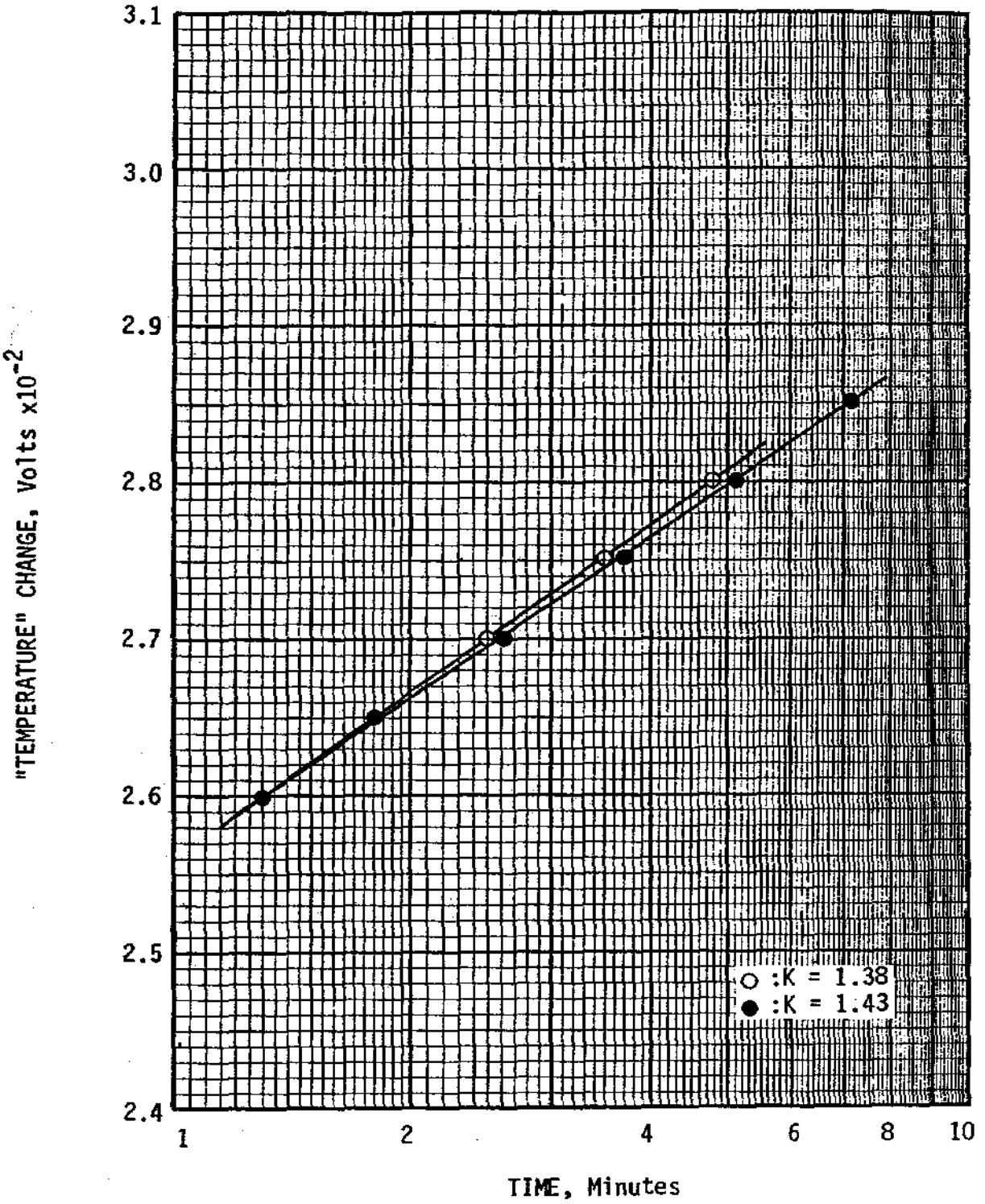

CLASSIFICATION SILTY SAND (SM)				**SOURCE** Boring 9 at 0.5'	
MOISTURE CONTENT 22.1 %		**DRY DENSITY** 105	pcf	□ FROZEN / ■ THAWED **THERMAL CONDUCTIVITY** 1.41	Btu / Ft-hr-°F
LL -- %	**PL** -- %	**-200 sieve** ---	%	**ORGANIC CONTENT** -----	%

Harding Lawson Associates
Engineers, Geologists
& Geophysicists

Thermal Conductivity
Pt. Thomson Development Project
Winter 1982, Geotechnical Study
Exxon Company, U.S.A.

PLATE **D-154**

DRAWN	JOB NUMBER	APPROVED	DATE	REVISED	DATE
	9612,031.08	DEB	4/82		

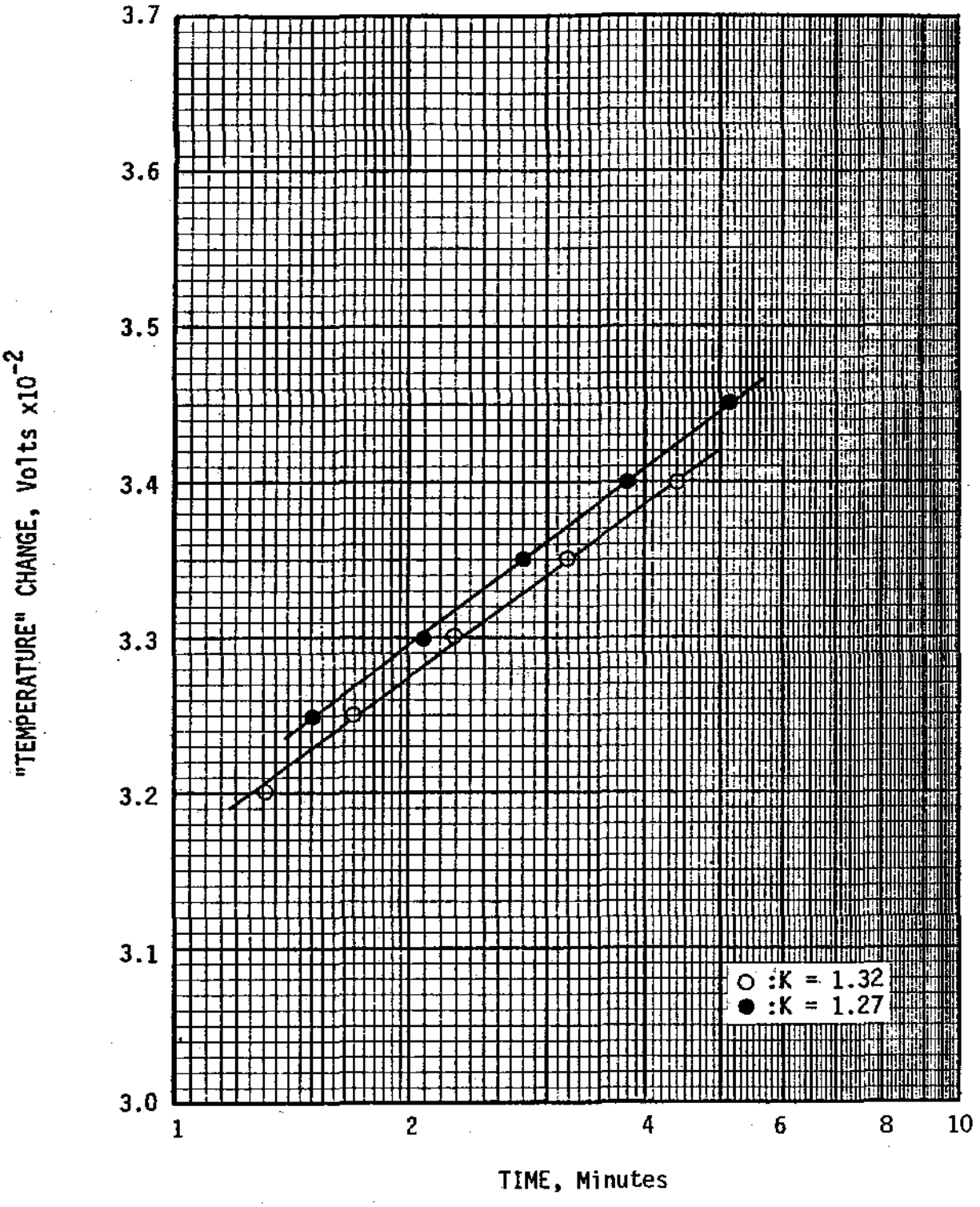

CLASSIFICATION SILTY CLAY (CL)				**SOURCE** Boring 9 at 46.4'	
MOISTURE CONTENT 29.3 %	**DRY DENSITY** 93	pcf	☐ FROZEN / ■ THAWED **THERMAL CONDUCTIVITY** 1.30	Btu / Ft-hr-°F	
LL -- %	**PL** -- %	**-200 sieve** --- %	**ORGANIC CONTENT** ----- %		

Harding Lawson Associates
Engineers, Geologists & Geophysicists

Thermal Conductivity
Pt. Thomson Development Project
Winter 1982, Geotechnical Study
Exxon Company, U.S.A.

PLATE **D-155**

DRAWN	JOB NUMBER	APPROVED	DATE	REVISED	DATE
JP	9612,031.08	DGB	4/82		

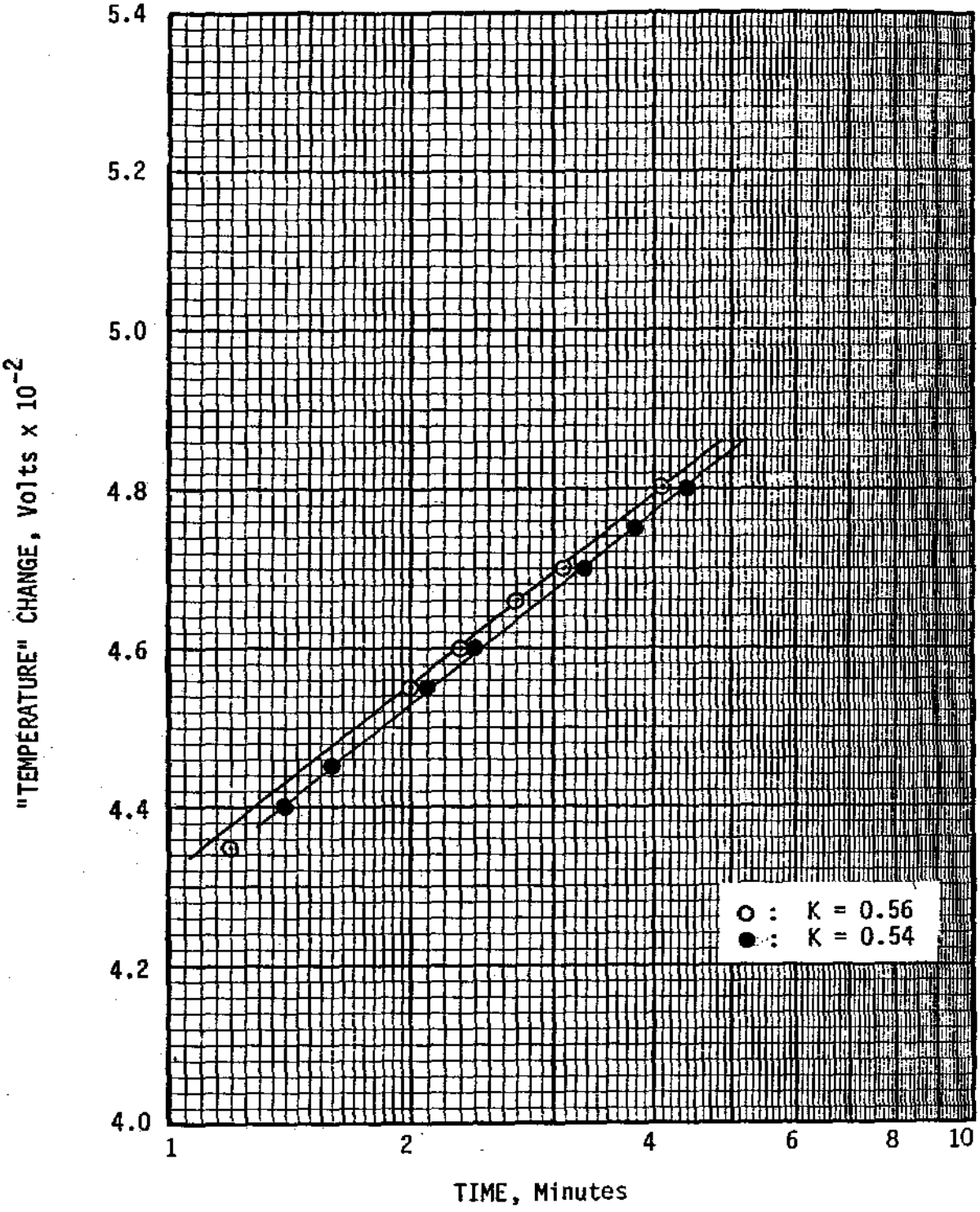

CLASSIFICATION ORGANIC SILT (OL,V_X/V_r)				**SOURCE** Boring 12 at 0.0'			
MOISTURE CONTENT 406	%	**DRY DENSITY**	11 pcf	■ **FROZEN** / □ **THAWED THERMAL CONDUCTIVITY**	0.55	Btu / Ft-hr-°F	
LL --	%	**PL** --	%	**-200 sieve** --	%	**ORGANIC CONTENT** --	%

Harding Lawson Associates
Engineers, Geologists & Geophysicists

Thermal Conductivity

Pt. Thomson Development Project
Winter 1982, Geotechnical Study
EXXON Company, U.S.A.

PLATE **D-156**

DRAWN	JOB NUMBER	APPROVED	DATE	REVISED	DATE
JP	9612,031.08	DEB	4/82		

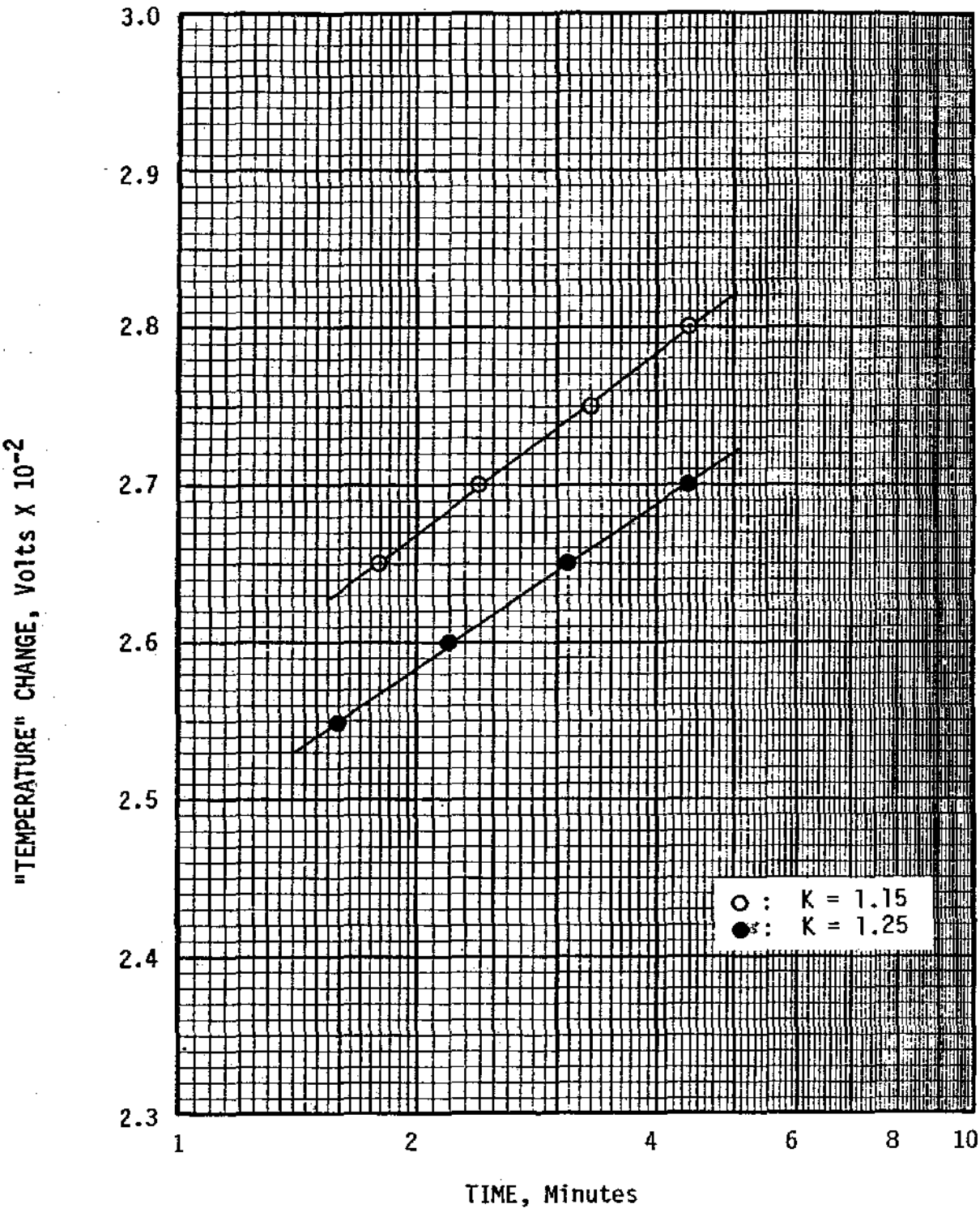

CLASSIFICATION CLAYEY SILT ($ML, V_X/V_Y$)		**SOURCE** Boring 13 at 18.0'	
MOISTURE CONTENT 154 %	**DRY DENSITY** 29 pcf	■ **FROZEN** / □ **THAWED THERMAL CONDUCTIVITY** 1.20	Btu / Ft-hr-°F
LL 34 % **PL** 25 %	**-200 sieve** -- %	**ORGANIC CONTENT** --	%

Harding Lawson Associates
Engineers, Geologists & Geophysicists

Thermal Conductivity
Pt. Thomson Development Project
Winter 1982, Geotechnical Study
EXXON Company, U.S.A.

PLATE **D-157**

DRAWN	JOB NUMBER	APPROVED	DATE	REVISED	DATE
JP	9612,031.08	DEB	4/82		

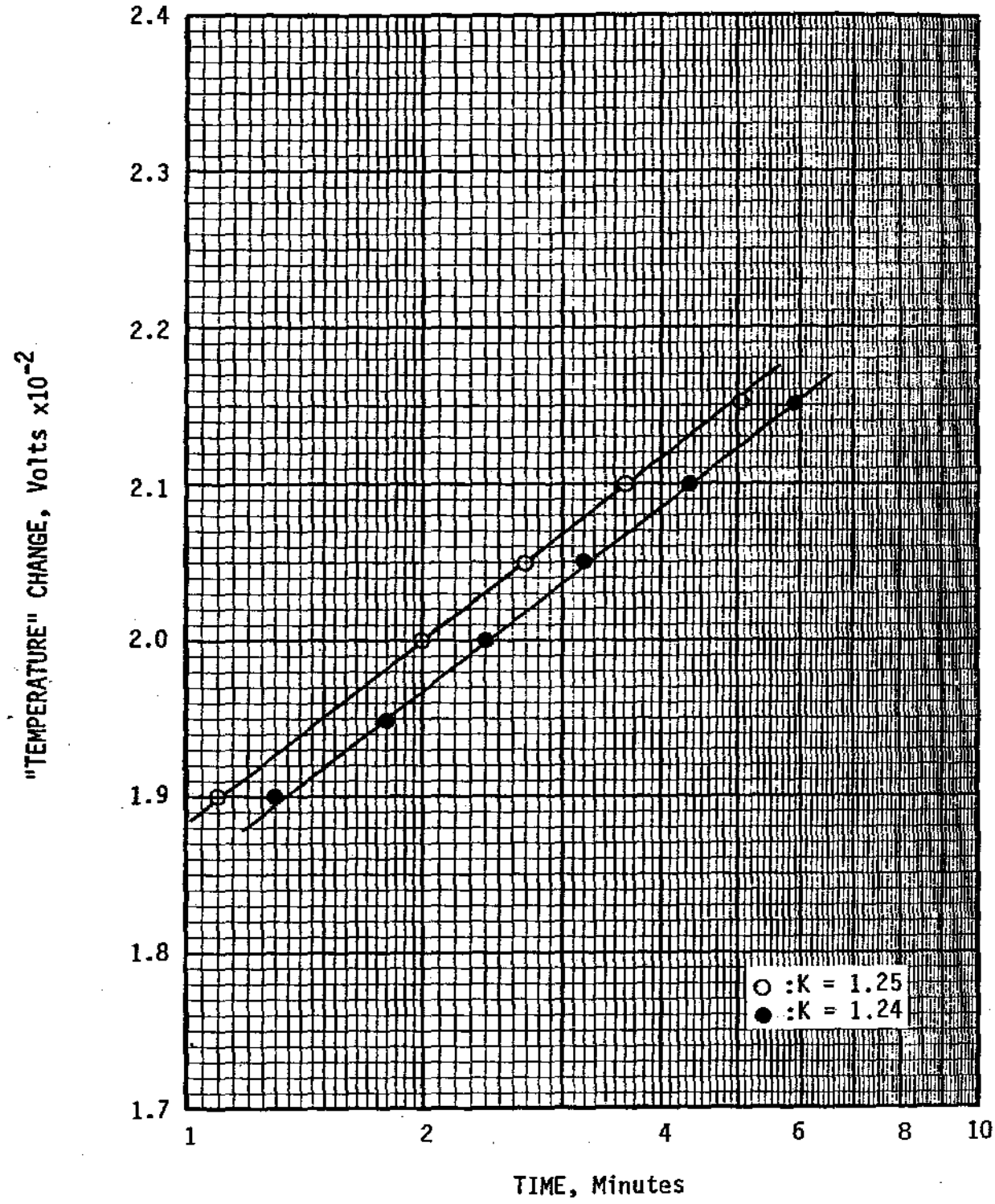

CLASSIFICATION SILTY CLAY (CL)				**SOURCE** Boring 14 at 31.1'	
MOISTURE CONTENT 22.8 %	**DRY DENSITY** 105	pcf	☐ FROZEN / ■ THAWED **THERMAL CONDUCTIVITY** 1.24		Btu / Ft-hr-°F
LL -- %	**PL** --- %	**-200 sieve** ---	%	**ORGANIC CONTENT** -----	%

Harding Lawson Associates
Engineers, Geologists & Geophysicists

Thermal Conductivity

Pt. Thomson Development Project
Winter 1982, Geotechnical Study
Exxon Company, U.S.A.

PLATE **D-158**

DRAWN	JOB NUMBER	APPROVED	DATE	REVISED	DATE
	9612,031.08	DEB	4/82		

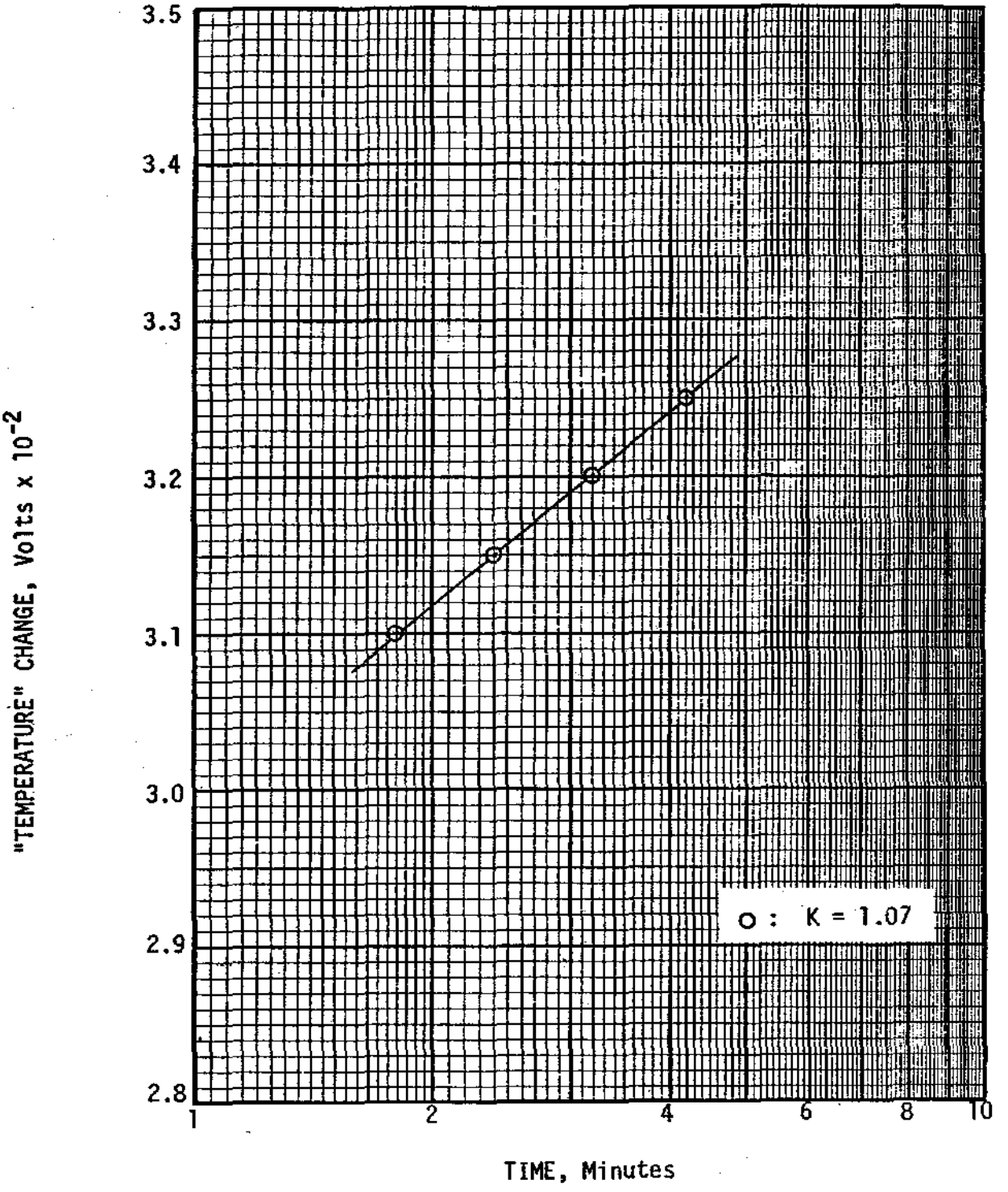

CLASSIFICATION ORGANIC SILT (OL, bonded)				**SOURCE** Boring 18 at 0.3'			
MOISTURE CONTENT 149%		**DRY DENSITY** 31	pcf	■ **FROZEN** / □ **THAWED THERMAL CONDUCTIVITY** 1.07		Btu / Ft-hr-°F	
LL --	%	**PL** --	%	**-200 sieve** --	%	**ORGANIC CONTENT** --	%

Harding Lawson Associates
Engineers, Geologists
& Geophysicists

Thermal Conductivity
Pt. Thomson Development Project
Winter 1982, Geotechnical Study
EXXON Company, U.S.A.

PLATE **D-159**

DRAWN	JOB NUMBER	APPROVED	DATE	REVISED	DATE
	9612,031.08	DEB	4/82		

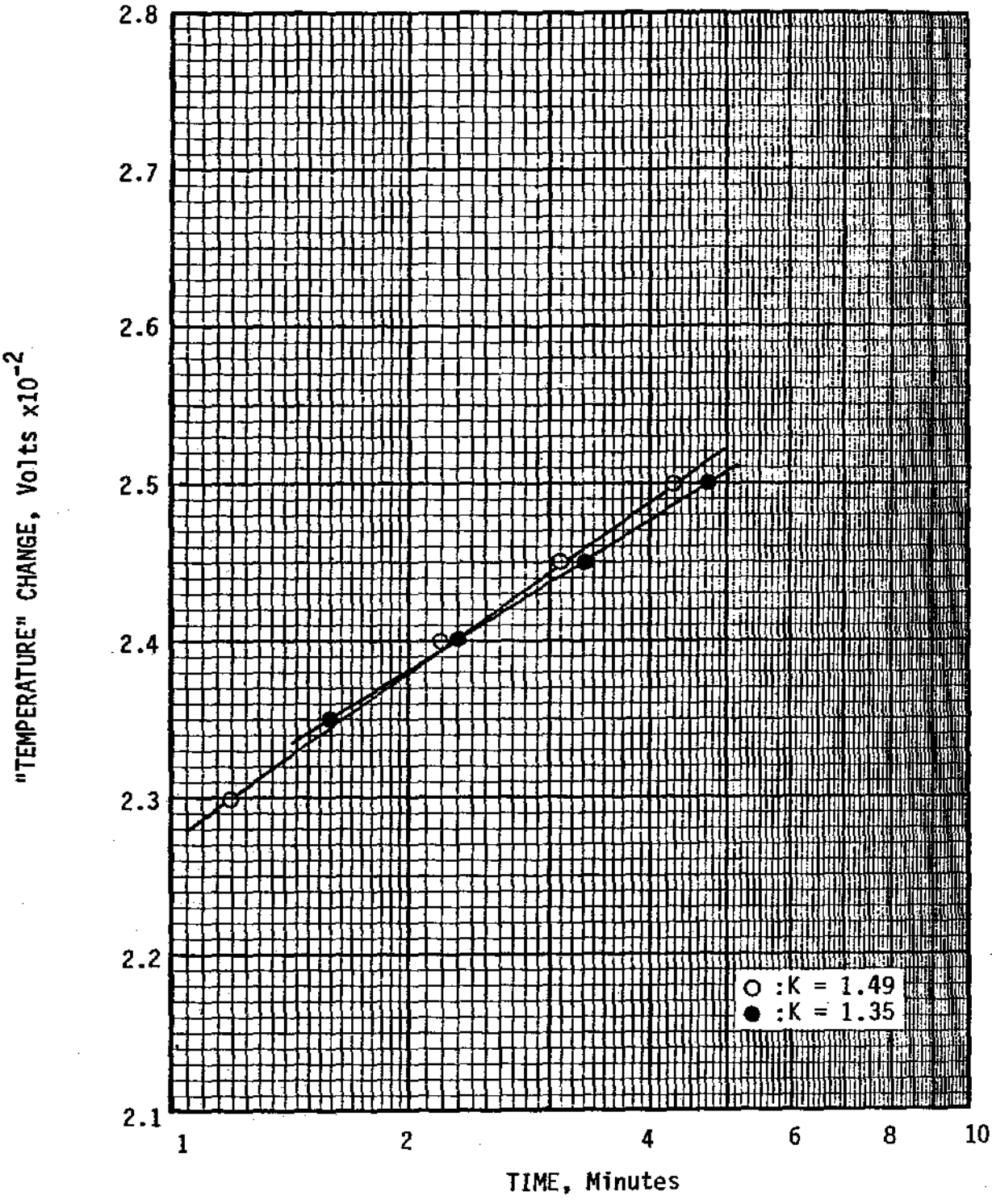

CLASSIFICATION SANDY SILT (ML)				**SOURCE** Boring 21 at 16.1'	
MOISTURE CONTENT 27.3 %	**DRY DENSITY** 97 pcf			□ **FROZEN** / ■ **THAWED** **THERMAL CONDUCTIVITY** 1.42	Btu / Ft-hr-°F
LL -- %	**PL** -- %	**-200 sieve** --- %		**ORGANIC CONTENT** ----- %	

Harding Lawson Associates
Engineers, Geologists & Geophysicists

Thermal Conductivity

Pt. Thomson Development Project
Winter 1982, Geotechnical Study
Exxon Company, U.S.A.

PLATE

D-160

DRAWN	JOB NUMBER	APPROVED	DATE	REVISED	DATE
	9612,031.08		4/82		

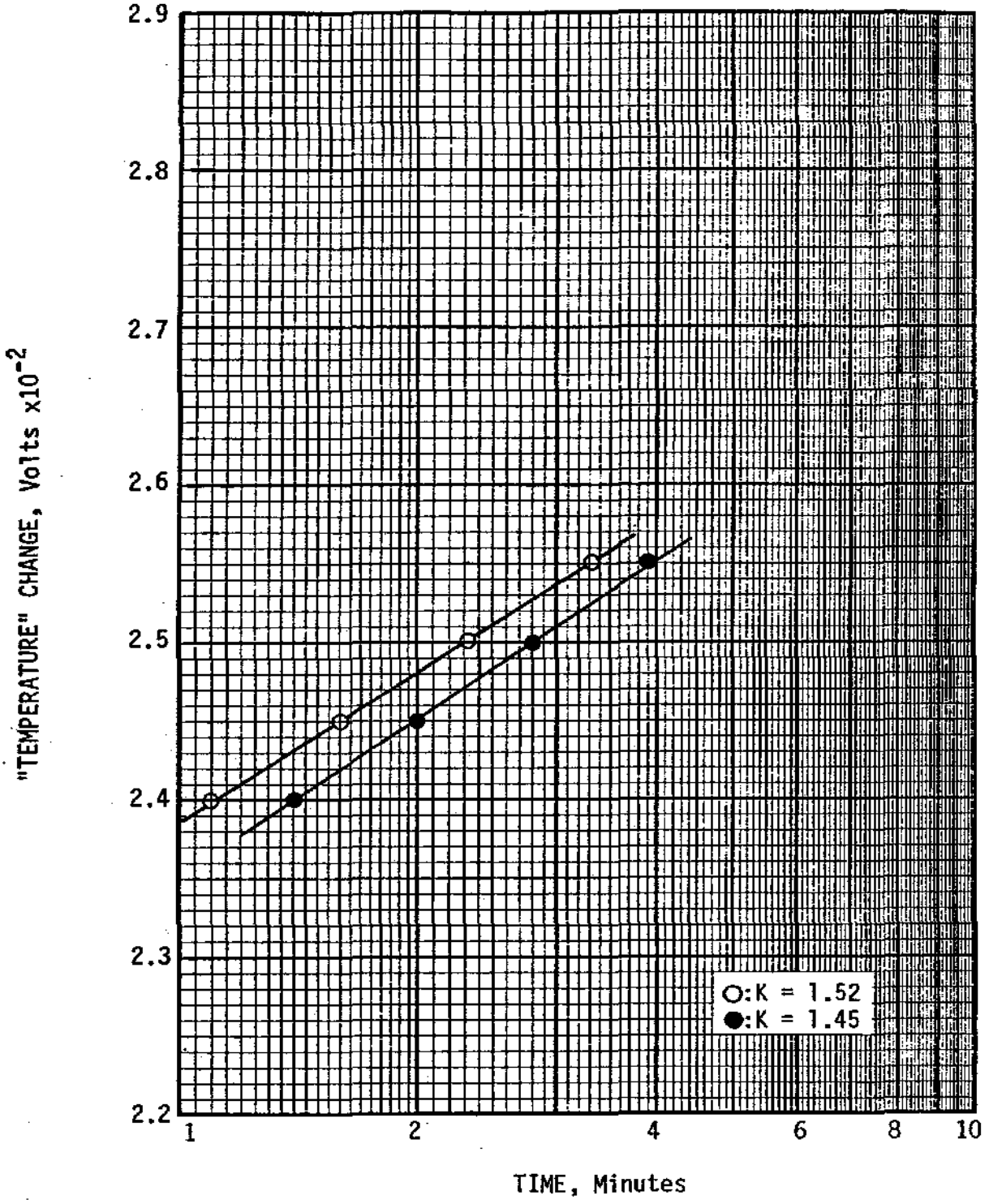

CLASSIFICATION CLAY (CL)			**SOURCE** Boring 21 at 31.0'
MOISTURE CONTENT 24.4 %	**DRY DENSITY** 101 pcf	☐ FROZEN / ■ THAWED **THERMAL CONDUCTIVITY** 1.49	Btu / Ft-hr-°F
LL -- %	**PL** -- %	**-200 sieve** --- %	**ORGANIC CONTENT** ----- %

Harding Lawson Associates
Engineers, Geologists & Geophysicists

Thermal Conductivity
Pt. Thomson Development Project
Winter 1982, Geotechnical Study
Exxon Company, U.S.A.

PLATE **D-161**

DRAWN	JOB NUMBER	APPROVED	DATE	REVISED	DATE
SP	9612,031.08	DEB	4/82		

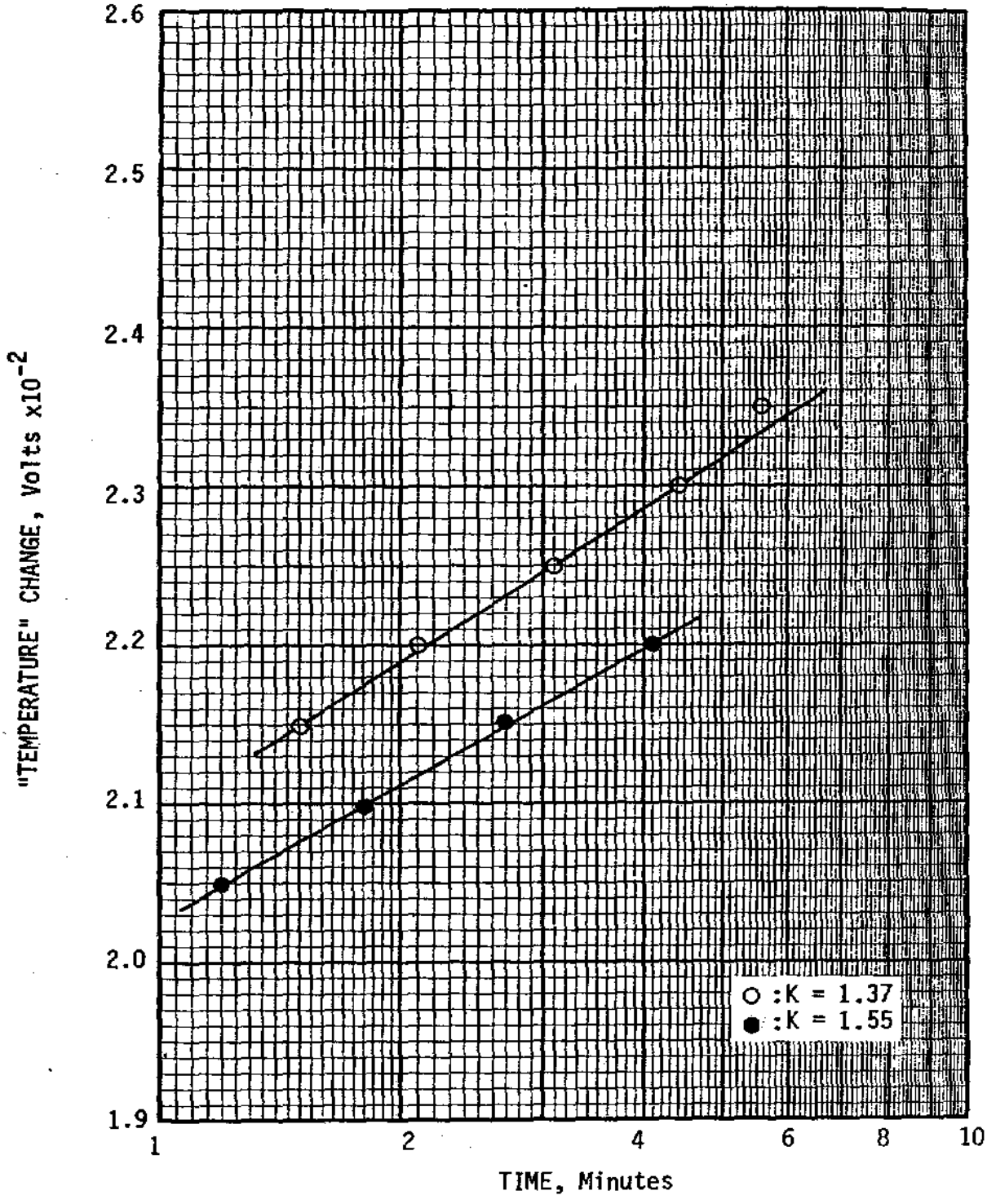

CLASSIFICATION SILT (ML, V_x)				**SOURCE** Boring 23 at 0.5'	
MOISTURE CONTENT 30.3 %	**DRY DENSITY** 78 pcf			■ **FROZEN** / □ **THAWED** **THERMAL CONDUCTIVITY** 1.46	Btu / Ft-hr-°F
LL --- %	**PL** --- %	**-200 sieve** ---- %		**ORGANIC CONTENT** ----	%

Harding Lawson Associates
Engineers, Geologists & Geophysicists

Thermal Conductivity

Pt. Thomson Development Project
Winter 1982, Geotechnical Study
Exxon Company, U.S.A.

PLATE D-162

DRAWN	JOB NUMBER	APPROVED	DATE	REVISED	DATE
JP	9612,031.08	DEB	4/82		

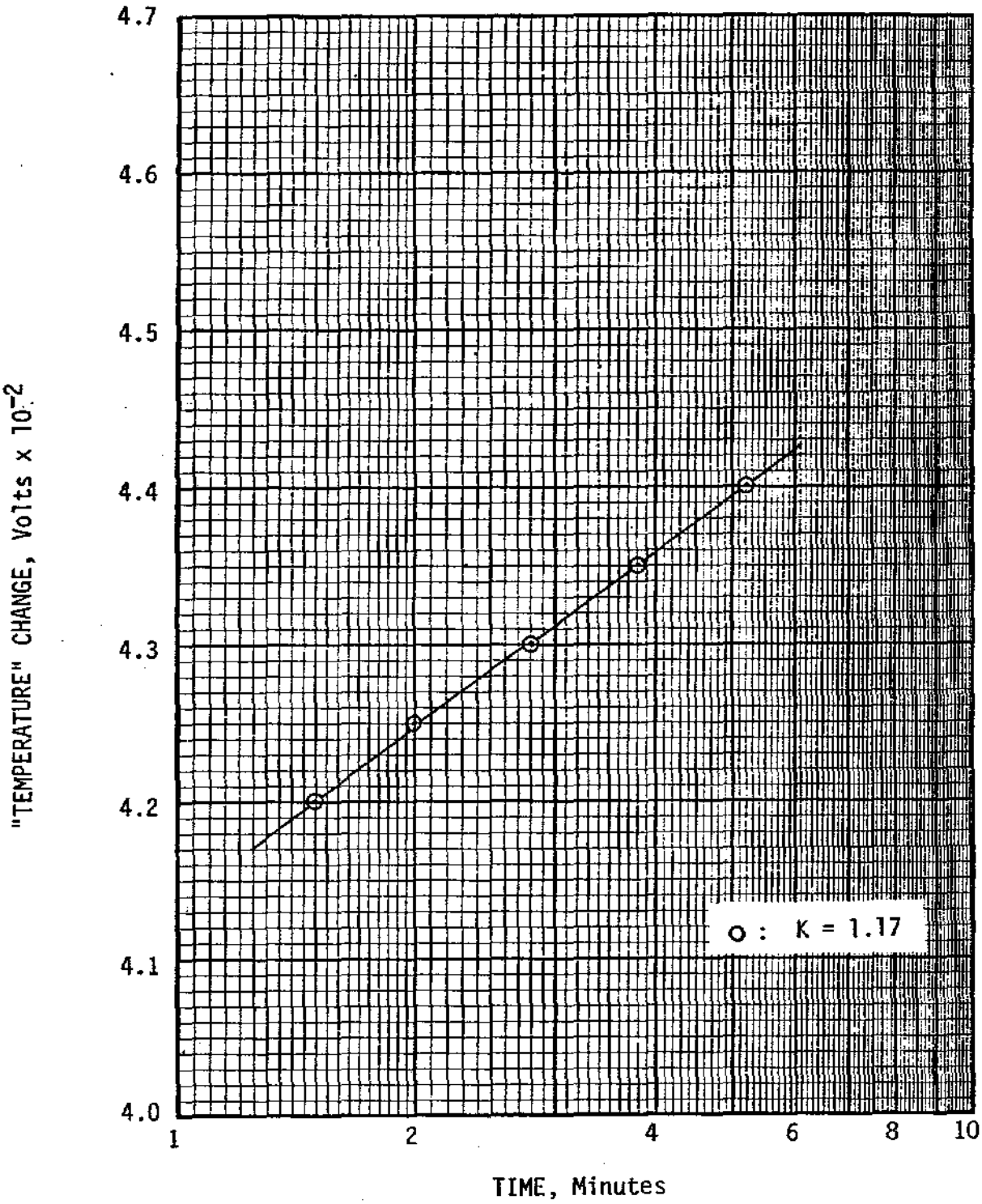

CLASSIFICATION SILTY CLAY (CL, V_f)				**SOURCE** Boring 23 at 12.5'	
MOISTURE CONTENT 43.9%	**DRY DENSITY** 70 pcf			■ **FROZEN** / □ **THAWED THERMAL CONDUCTIVITY** 1.17	Btu / Ft-hr-°F
LL 33 %	**PL** 22 %	**-200 sieve** -- %		**ORGANIC CONTENT** --	%

Harding Lawson Associates
Engineers, Geologists
& Geophysicists

Thermal Conductivity
Pt. Thomson Development Project
Winter 1982, Geotechnical Study
EXXON Company, U.S.A.

PLATE
D-163

DRAWN	JOB NUMBER	APPROVED	DATE	REVISED	DATE
SF	9612,031.08	DEB	4/82		

was performed on silty sand (SM), the value obtained was higher than values recorded for the fine-grained soils. We observed no substantial difference between the clays, silts, and organic silts.

On Plate IV-24, thermal conductivities from this study are plotted against thermal conductivities from Kersten's work (1949). It can be observed that the thawed thermal conductivities of Beaufort Sea soils are greater than those predicted by Kersten's values. From the limited data developed during this study, it appears that the frozen thermal conductivities agree with Kersten's values.

APPENDIX E
EXPLANATION OF ANALYTICAL PROCEDURES

APPENDIX E
EXPLANATION OF ANALYTICAL PROCEDURES

This appendix contains detailed discussions of the methods used to define the mechanical properties of fill materials as presented in the Duck Island Development (DID) report (HLA, 1981), the methods used to define pile settlement and the analysis of laterally loaded piles in permafrost. Subsurface soil and gravel fill materials from the DID area are similar to those found in the PTD area; consequently, the relationships and analytical procedures used in the DID study are applicable to this study.

A. MECHANICAL PROPERTIES OF FILL MATERIALS

1. MECHANICAL PROPERTIES OF UNBONDED FILL MATERIALS

Both materials placed in the summer and gravel-ice mixtures placed in the winter will behave as unbonded soils until freezeback of free pore water. The parameters governing the behavior of fill materials in the unbonded condition include elastic modulus and Poisson's ratio, shear strength and compressibility. Estimated values for these parameters, based on index properties, laboratory test data and correlations available in the literature for similar soil types, are presented in Table IV-6.

Table IV-6. Mechanical properties of unbonded fill material

	[1] Initial Tangent Modulus		Poisson's Ratio μ	Shear Strength		[2] One Dimensional Compression Modulus	
				Friction Angle ϕ	[3] Cohesion c, psi		
	k	n				m	a
Ice-Free Gravel							
Placed in the dry, compacted to R_d = 0.7	250	0.4	0.30	40°	0	1000	0.9
Placed below sea level, R_d = 0.5	200	0.4	0.30	36°	0	800	0.9
Gravel-Ice Mixtures							
Placed in the dry, compacted	100	0.4	0.30	20°	0	400	0.75
Placed below sea level	60	0.4	0.35	15°	5	230	0.50
Silty Sands-Hydraulic Fill							
uncompacted, R_d = 0.3	75	0.25	0.45	28°	0	40	0.10
compacted, R_d = 0.7	150	0.25	0.45	32°	0	80	0.25

1. $E_i = \left(\frac{\sigma_1-\sigma_3}{\epsilon_1}\right)_i = k\ P_a \left(\frac{\sigma_3}{P_a}\right)^n$ (After Duncan et.al., 1980)

2. $M = \frac{\sigma_1}{\epsilon_1} = m\ P_a \left(\frac{\sigma_1}{P_a}\right)^{1-a}$ (After Janbu, 1967)

where: P_a = atmospheric pressure in same unit as σ_1 and σ_3

3. All unbonded fill materials considered cohesionless, except gravel-ice mixtures for which a nominal cohesion is assigned to account for some ice bonding when very cold gravel-ice mixtures are deposited underwater.

The shear strength is represented by the Mohr-Coulomb failure criterion:

$$s = c + \sigma_n \tan\phi \qquad \text{(IV-8)}$$

where: s = shear strength
c = cohesion intercept
σ_n = normal stress on the failure plane
ϕ = angle of internal friction

The elastic moduli are presented as initial tangent moduli (E_i) in the form (Duncan et al., 1980):

$$E_i = \left(\frac{\sigma_1 - \sigma_3}{\epsilon_1}\right)_i = k(P_a)\left(\frac{\sigma_3}{P_a}\right)^n \qquad \text{(IV-9)}$$

where: σ_1, σ_3 = major and minor principal stresses, respectively
ϵ_1 = major principal strain
k = modulus number
n = modulus exponent
P_a = atmospheric pressure

Assuming a hyperbolic stress-strain relationship, the tangent modulus, E_t, for any stress condition, $(\sigma_1 - \sigma_3), \sigma_3$, can be computed from

$$E_t = \left[1 - \frac{R_f(1-\sin\phi)(\sigma_1-\sigma_3)}{2c(\cos\phi) + 2\sigma_3(\sin\phi)}\right] E_i \qquad \text{(IV-10)}$$

where: R_f = "failure ratio" $\approx$ 0.7 for moist soils

Similarly, compressibility is presented in terms of the one-dimensional modulus (M), i.e.,

$$M = \frac{d\sigma_v}{d\epsilon_v} = m(P_a)\left(\frac{\sigma_v}{P_a}\right)^{1-a} \qquad \text{(IV-11)}$$

in which σ_v and ϵ_v are the vertical stress and strain in one-dimensional compression, "m" is the modulus number, "a" is the stress exponent, and "P_a" is atmospheric pressure (Janbu, 1967).

2. MECHANICAL PROPERTIES OF BONDED FILL MATERIALS

Lacking reliable experimental data, the following discussion presents methods for qualitative assessment of the mechanical properties of bonded fill material. Direct measurements are needed to evaluate the validity of these methods and the results and conclusions derived from them.

a. Creep and Strength Properties of Bonded Fill Materials

The stress-strain-time behavior of bonded fill materials will be influenced by several material and environmental variables, of which the following could have a significant effect:

- Material type; i.e., silt, sand, or gravel
- Strain rate ($\dot{\epsilon}$)
- Temperature (θ)
- Void ratio (e)
- Ice saturation (S_i)
- Brine content (S_b)
- Confining pressure (σ_3)

Functionally, we may express the stress-strain-time relationship for a given material type as:

$$\sigma = \sigma (\dot{\epsilon}, t, \theta, R_d, S_i, S_b, \sigma_3) \qquad \text{(IV-12)}$$

where: $\sigma = \sigma_1 - \sigma_3$ = deviator stress

$\dot{\epsilon} = \frac{d\epsilon}{dt}$ = strain rate

t = time

Ladanyi (1972) has proposed the following creep law:

$$\dot{\epsilon} = \dot{\epsilon}_c \left(\frac{\sigma}{\sigma_c}\right)^n \qquad \text{(IV-13a)}$$

$$\sigma = \sigma_c \left(\frac{\dot{\epsilon}}{\dot{\epsilon}_c}\right)^{1/n} \qquad \text{(IV-13b)}$$

where: σ = applied stress
σ_c = creep modulus (a reference stress)
$\dot{\epsilon}$ = strain rate resulting from applied stress, σ
$\dot{\epsilon}_c$ = strain rate corresponding to stress, σ_c
n = creep exponent

This form of creep law assumes that steady-state creep dominates. It is assumed that primary (attenuating) creep is insignificant in comparison to steady-state creep and that the creep rate does not accelerate (tertiary creep) within the duration of loading being considered. The implication of these assumptions is illustrated on Figure IV-9.

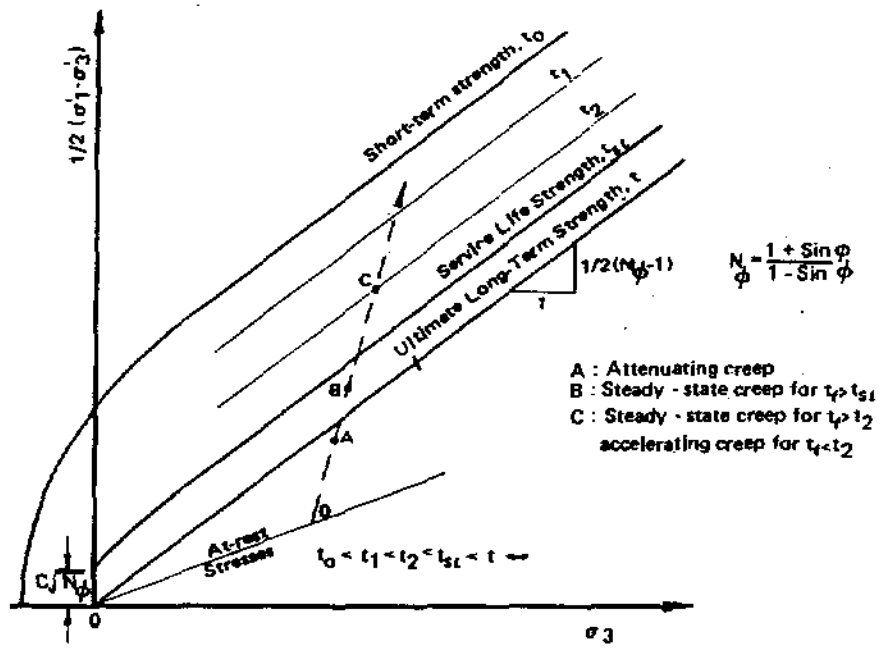

Figure IV- 9 Strength versus time behavior for frozen soils (modified after Ladanyi, 1975).

The strength of a frozen soil under various durations of loading are shown in $\frac{1}{2}(\sigma_1 - \sigma_3) : \sigma_3$ stress space on Figure IV-9. The frictional component of the frozen strength (represented by the slope of the failure envelopes) is assumed to be independent of time whereas the cohesion component (the shear strength when the confining pressure, σ_3, is zero) decreases with time and eventually vanishes when time becomes infinite.

The line OABC represents a hypothetical loading path starting from at-rest conditions (point O). Because the loading represented by OA never exceeds the ultimate long-term strength, the creep rate decreases with time and eventually stops. This is the case of attenuating creep. On the other hand, the loading OC exceeds the service life strength; failure by tertiary creep will occur at time t_2 before the service life is reached.

Loading 08 exceeds the ultimate long-term strength but is less than the service life strength. It is this type of loading condition for which Equation (IV-13a,b) is assumed to be valid. The requirements for validity of the creep law are as follows:

$$\sigma_{ult} < \sigma_{app} < \sigma_{sl} \qquad \text{(IV-14)}$$

where: σ_{ult} = ultimate long-term creep strength
σ_{app} = applied stress
σ_{sl} = service life creep strength

As a practical matter, these requirements are usually satisfied because, on the one hand, proper design cannot permit the applied stress to exceed the service life creep strength and, on the other hand, the ultimate long-term (frictional) strength is generally quite low, except in the case of dense, ice-poor soils.

It is assumed that the effects of the material and environmental variables previously identified can be approximately accounted for in the creep modulus term

$$\sigma_c = \sigma_c\ (\theta,\ e\ ,\ S_i,\ S_b,\ \sigma_3) \qquad \text{(IV-15)}$$

The effects of each of the variables are discussed below:

(1) Temperature

The qualitative effects of temperature on the creep behavior of frozen soils are well known. In general, as the temperature decreases, the creep rate decreases and the creep strength increases. The quantitative functional relationships are less well established, but generally seem to be of the form suggested by Sayles and Haines (1974):

$$\left(\frac{\sigma_\theta}{\sigma_0}\right)=\left(\frac{\theta}{\theta_0}\right)^m \qquad \text{(IV-16)}$$

in which, σ_θ and σ_0 are stresses (or strengths) at temperatures of θ and θ_0 (^{0}F below freezing) and m is the temperature exponent. Figure IV-10 shows peak strength versus temperature data reported by Sayles and Haines (1974) for ice and four different types of soil.

For the four different soil types the temperature exponent, m, varies within fairly narrow limits, i.e., m = 0.48 ± 15 percent. Therefore, we have assumed that m = 0.5 can be used for the soil types expected to be used as fill for this project. The possible dependency of m on salinity is assumed to be accounted for by the brine content factor discussed below.

(2) Void Ratio

Goughnour and Andersland (1968) found that the shear strength of frozen Ottawa sand varies considerably with the volume concentration of sand in a sand-ice mixture. Sand concentration is defined as the ratio of sand volume to total volume; thus, sand concentration = 1/(1 + e). As the sand concentration was varied from zero (pure ice) to about 42 percent (e = 1.38), only a minor increase in the shear strength was observed. However, above 42 percent, the shear strength increases rapidly, continuing up to a sand concentration of about 63 percent (e = 0.59). Linell and Lobacz (1980) have presented data for Manchester fine sand that show a peak strength at an "ice content" of about 0.58, with the strength decreasing for both higher and lower ice contents. (Note: "ice content" is defined by Linell and Lobacz as the volumetric ratio of ice to soil, which is equivalent to void ratio for 100 percent ice saturation).

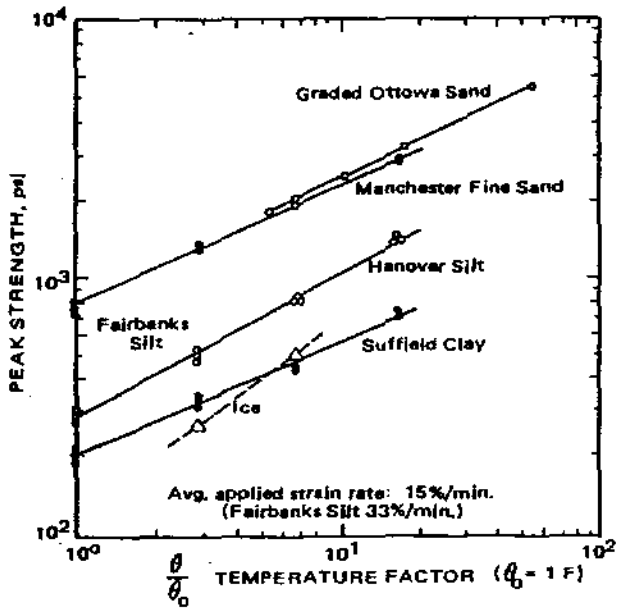

$$\left(\frac{\sigma_\theta}{\sigma_0}\right) = \left(\frac{\theta}{\theta_0}\right)^m$$

Soil	σ_0 (psi)	m
Graded Ottawa sand	789	0.48
Manchester fine sand	812	0.44
Hanover silt	288	0.55
Suffield clay	204	0.43
	Avg.=	0.48

Figure IV-10. Peak Strength vs. Temperature (After Sayles and Haines, 1974)

If the data of Goughnour and Andersland (1968) and Linell and Lobacz are normalized with respect to peak strength and plotted as a function of void ratio, the data appear as shown in Figure IV-11. Figure IV-11 also shows the relative strength reduction that can be expected for the various fill material types being considered for this project. These reduction factors must be considered as only rough approximations since there are no corroborating test data for the materials.

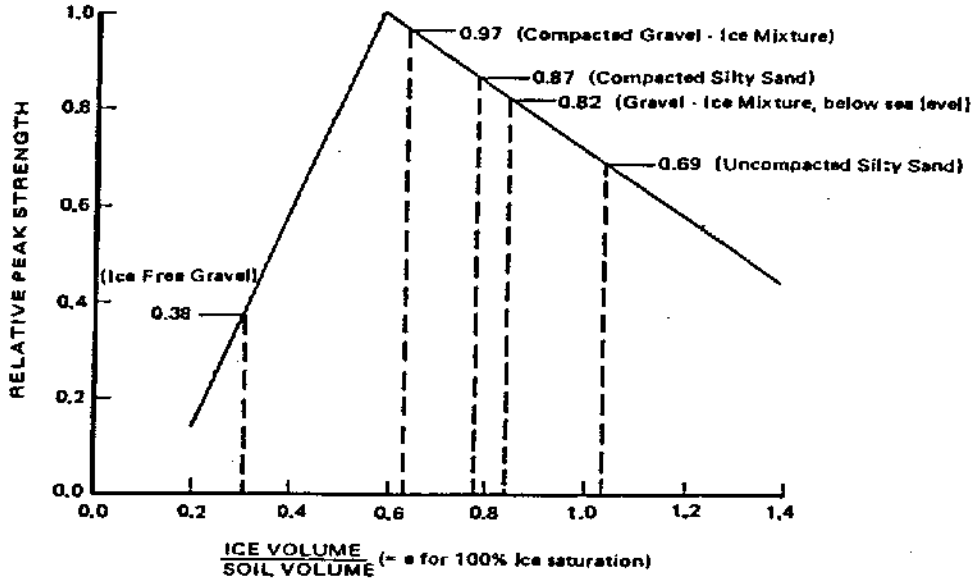

Figure IV-11. Variation of peak strength with volumetric ice content (Data from Linell and Lobacz, 1980 and Goughnour and Andersland, 1968)

(3) Ice Saturation

Alkire and Andersland (1973) have addressed the effects of ice saturation on frozen Ottawa sand-ice mixtures. Their data, reproduced in Figure IV-12, show a reduction in strength with reduction in ice saturation. Since only two values of ice saturation were used in their study, linear interpolation and extrapolation were used to develop approximate relationships. Extrapolation was confined to ice saturation in the range of 0.18 S_i 1.00 because the curve for zero confining pressure indicates zero strength for S_i 0.18.

If the data in Figure IV-12 are normalized with respect to peak strength at S_i = 1.0 and the effect of confining pressure omitted, the relationship in Equation IV-17 results.

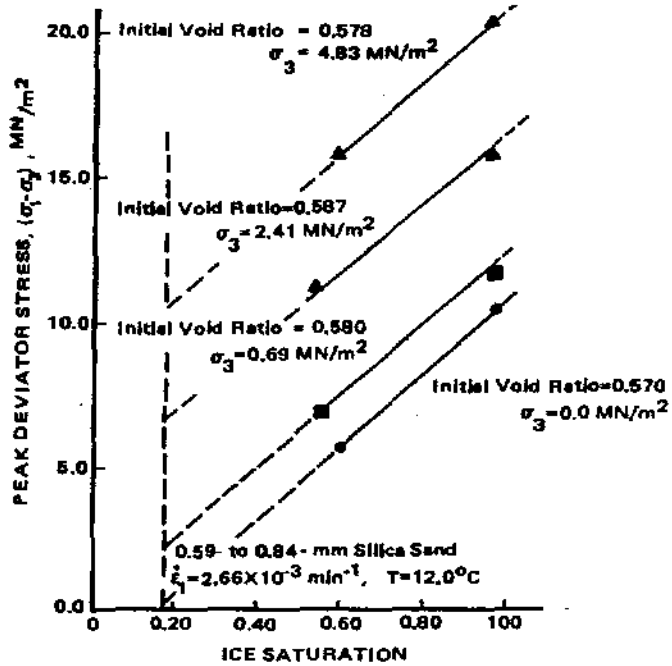

Figure IV-12 Peak deviator stress versus ice saturation for various confining pressures (After Alkire and Andersland, 1973).

The effects of confining pressure are quite apparent in Figure IV-12; this factor will be discussed below. Again, the data on the effects of ice saturation described above are for one material type only, Ottawa sand, and applying the effects to gravels and silty sands involves considerable uncertainty.

$$\frac{\sigma_{Si}}{\sigma_{Si=1.0}} = -0.22 + 1.22\,S_i \quad \left\{ \text{for} \quad \begin{matrix} 0.18 \le S_i \le 1.0 \\ \sigma_3 = 0 \end{matrix} \right\} \qquad \text{(IV-17)}$$

(4) Brine Content

Fill materials from offshore sources or those from onshore sources placed below sea level will contain significant brine in the pore water. Michel (1978) has shown that brine content can have a substantial effect on the strength of sea ice. Michel's data, reproduced in Figure IV-13, show that the

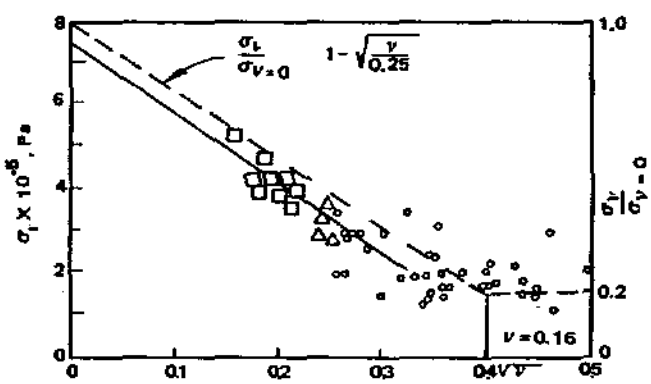

Figure IV-13. Flexure strength of sea ice vs. brine volume (After Michel, 1978).

flexural strength of sea ice is reduced to 20 percent of the strength of brine-free ice at a brine volume of about 0.16. At higher volumes, no further strength reduction occurs because the excess brine drains out of the ice. Michel suggests the following empirical relationship for strength reduction as a function of brine volume:

$$\frac{\sigma_\nu}{\sigma_{\nu=0}} = 1 - \sqrt{\frac{\nu}{0.25}} \qquad \left| \text{for } 0 \le \nu \le 0.16 \right| \qquad \text{(IV-18)}$$

Ruedrich and Perkins (1974) investigated the effect of salt concentration on the strength of Prudhoe Bay sands and silts. Some of their results are reproduced in Figure IV-14; substantial reductions in strength with increasing salt concentrations are readily apparent.

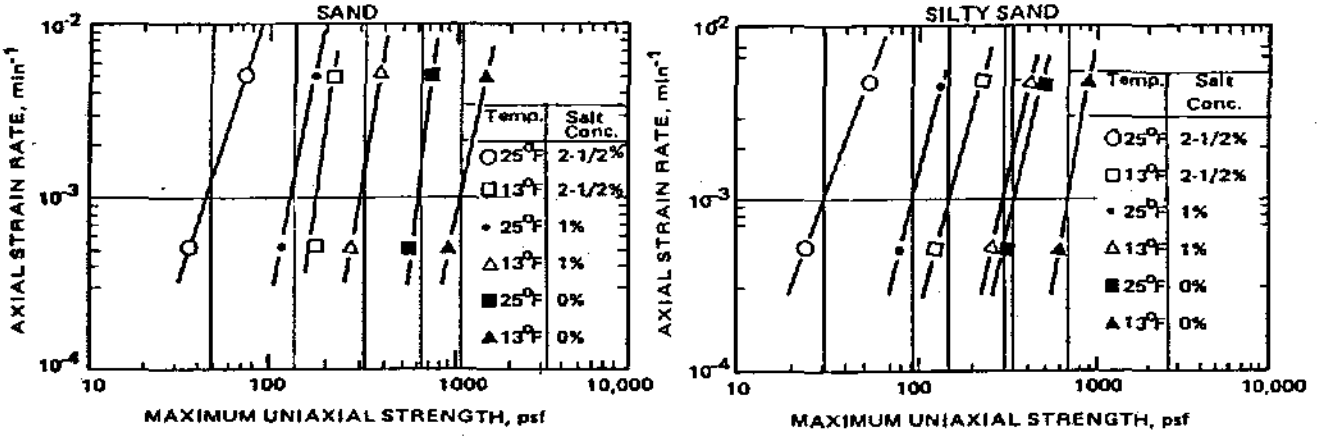

Figure IV-14. Influence of salt concentration on the strength of Prudhoe Bay sand and silty sand (After Ruedrich and Perkins, 1974).

In order to determine whether the influence of salt concentration in the frozen Prudhoe Bay sands and silty sands is similar to the effect of brine volume on sea ice, we have plotted the strength (at axial strain rate = 10^{-3} min^{-1}) from Figure IV-14 versus brine volume in the form used by Michel (1978) for sea ice. Brine volumes were estimated from the pore water salinity and test temperatures reported by Ruedrich and Perkins (1974) for the Prudhoe Bay samples. The results are shown in Figure IV-15.

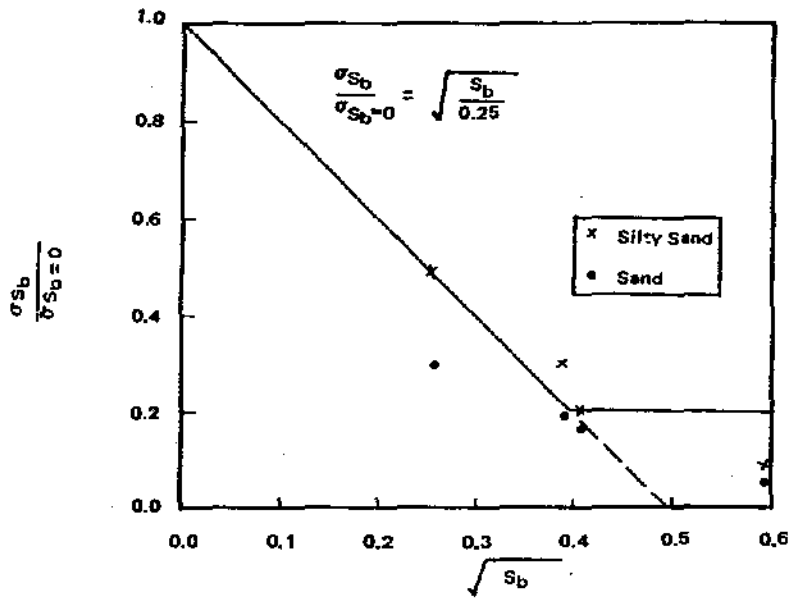

Figure IV-15. Influence of brine volume on the strength of Prudhoe Bay sand and silty sand (After Ruedrich and Perkins, 1974)

Although the data are limited, the relationship proposed by Michel (1978) appears to fit quite well. However, at brine volumes greater than 0.16, the data indicate that the strength continues to decrease because, in contrast to the natural freezing of sea ice, brine was not allowed to drain from the Prudhoe Bay test samples. It is our opinion that when the offshore fills freeze the brine will drain except possibly in the lowest portion of the fills, where brine may become trapped. For the case of gravel -ice mixtures placed below sea level, the brine volume is replaced by brine content to account for the initial freshwater ice content of the mixture (see Equation IV-5). Therefore, after replacing ν with S_b Equation IV-18 becomes:

$$\frac{\sigma_{S_b}}{\sigma_{S_b=0}} = 1 - \sqrt{\frac{S_b}{0.25}} \quad \{\text{for } 0 \leq S_b \leq 0.16\} \qquad \text{(IV-19)}$$

(5) Confining Pressure

To account for the effect of confining pressure on creep behavior, Ladanyi (1975) proposes to treat frozen soil as a (c, ϕ) material by replacing the creep modulus in Equation IV-13, σ_c by σ_{cf}, i.e.,

$$\sigma_{cf} = \sigma_c + \sigma_{3,av} \quad (N_\phi - 1) \qquad \text{(IV-20)}$$

where: $N_\phi = \frac{1+\sin\phi}{1-\sin\phi}$

$$\sigma_c = 2c\sqrt{N_\phi}$$

ϕ denotes the friction angle of the frozen soil corresponding to the creep rate, $\dot{\epsilon}_c$, and c is the cohesion intercept. In this approach, c and ϕ are total stress parameters and ϕ is assumed to be relatively independent of time and temperature.

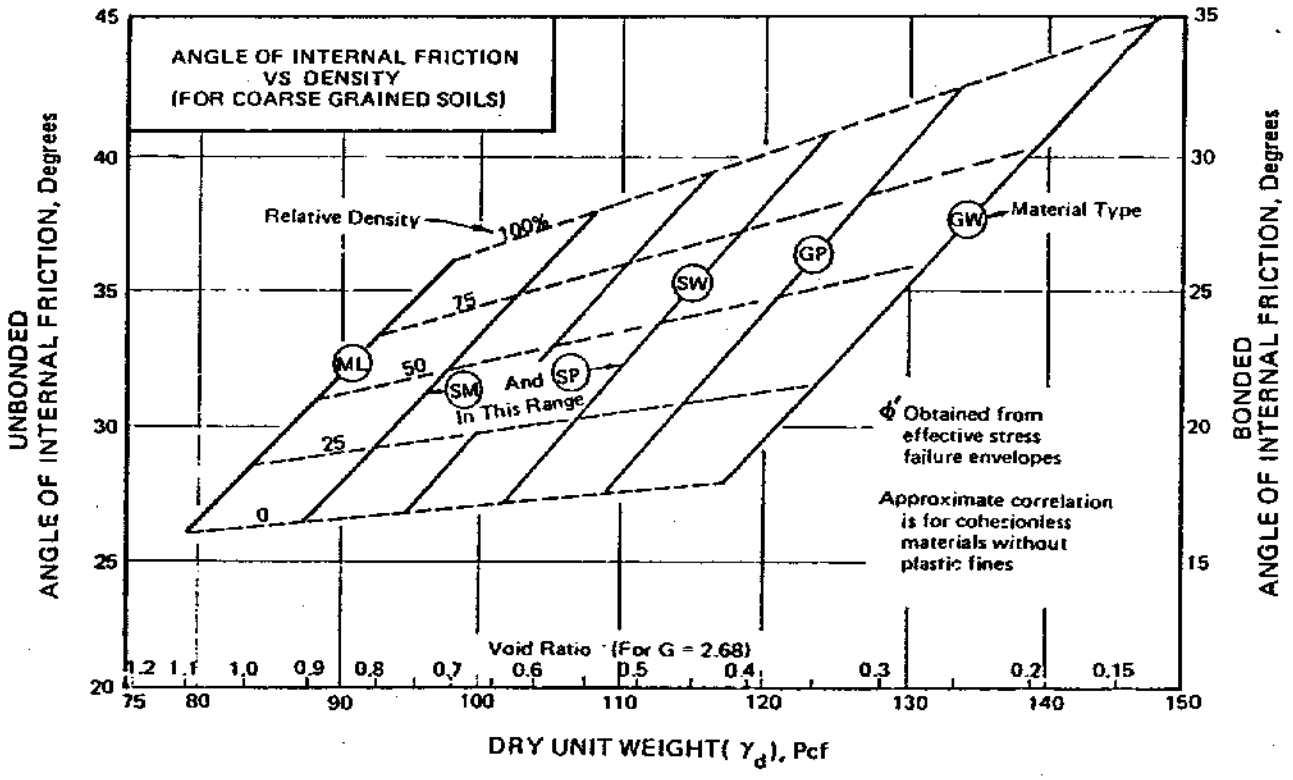

Figure IV-16. Angle of internal friction vs. density for frozen and unfrozen fill materials. Based on bonded angle of internal friction being 10 degrees less than the unbonded value (After Navdocks, 1971)

The angles of internal friction for ice-saturated frozen soils reported in the literature are typically six to ten degrees less than those for the same soil and density in the unfrozen condition (see, for example, Alkire and Andersland, 1973, Ladanyi and Johnston, 1973, and Sayles, 1973). If the difference in friction angles between the frozen and unfrozen state for the same soil and dry density is taken to be 10 degrees, the curves shown in Figure IV-16 can be used to estimate the friction angles for frozen fill materials.

The effects of temperature, void ratio, brine content in the pore fluid, ice saturation and confining pressure, as described in the preceeding discussion, can now be incorporated into the creep modulus, σ_c.

The parameters required to apply Equations IV-13 and IV-13b are as follows:

- Creep modulus, σ_c, and the corresponding strain rate, $\dot{\epsilon}_c$.
- Creep exponent, n
- Temperature factor, m (see Figure IV-10 and Equation IV-16)
- Index properties which influence the creep modulus
  - Void Ratio (e) (see Figure IV-11)
  - Ice saturation (S_i) (see Equation IV-17)
  - Brine content (S_b) (see Figure IV-15 and Equation IV-19)
  - Confining pressure σ_3 (see Figure IV-16 and Equation IV-20).

The index properties of the fill materials have been discussed previously and values for various typical conditions presented in Tables IV-4, IV-5, and IV-6. Representative values of creep modulus, creep exponents, and temperature factors are presented in Table IV-7.

The values of creep modulus are equivalent to the peak strength at a temperature of 31°F and a strain rate of 0.15 $min.^{-1}$ and are estimated from the data of Sayles and Haines (1974) shown in Figure IV-10.

TABLE IV-7. Summary of creep properties for bonded fill materials[1]

$\dot{\epsilon} = \dot{\epsilon}_c \left(\frac{\sigma}{\sigma_c}\right)^n$	Ice-Free Gravel	Gravel-Ice Mixtures		Ice-Free Silty Sands	
	placed below sea level (R_d = 0.5)	placed in the dry, compacted (Recrystalized)	placed below sea level, uncompacted	uncompacted (R_d = 0.3)	compacted (R_d = 0.7)
Creep Exponent, n	7.5	7.5	7.5	7.5	7.5
Creep Modulus, σ_c (ksf) (@ $\dot{\epsilon}_c = 0.15\ min^{-1}$)	115	[2]57	115	90	90
Adjustments to Creep Modulus					
(1) Temp. Exponent, m	0.5	0.5	0.5	0.5	0.5
Temp. factor	2.4	2.4	2.4	2.4	2.4
(2) Void Ratio Factor	0.38	0.97	0.87	0.69	0.87
(3) Ice Sat. Factor	—	0.34	—	—	—
(4) Brine Content	0.2	—	0.2	0.2	0.2
(5) Conf. Pressure Factor					
ϕ (degrees)	26	10	5	18	22
$(N_\phi - 1)$	1.56	0.42	0.19	0.89	1.20
Adjusted Creep Modulus	$21.0+1.56\sigma_3$	[2] $(45.0 + 0.42\sigma_3)$	$48.0 + 0.19\sigma_3$	$2.98+0.89\sigma_3$	$37.6 + 1.20\sigma_3$

Notes:

1. For average fill temperature = -5°C.
2. Depends upon degree of recrystallization.

The creep exponent was estimated from data on four different soil types ranging from Ottawa sand to Suffield clay (Sayles, 1968; Sayles and Haines, 1974). The values were obtained from Equation IV-13 rewritten as follows:

$$n = \frac{\log \left[\frac{\epsilon_f}{t_{100}\ \dot{\epsilon}_c} \right]}{\log \left[\frac{\sigma_{f100}}{\sigma_{pk}} \right]} \qquad \text{(IV-21)}$$

Where, ϵ_f = failure strain
t_{100} = 100 years
σ_{pk} = short-term creep strength
$\dot{\epsilon}_c$ = strain rate for σ_{pk}
σ_{f100} = creep strength at 100 years

Values of n were computed for several pairs of data at the same temperature for each soil type. In general, the computed n-values decreased with increasing temperatures, but varied little with soil type. A value of n = 7.5 was selected as representative of the range of soil types reported for temperatures of 25^0 to 31^0F. This is believed to be a conservative value for the project fill materials.

Using the data presented in Table IV-7 and Equation IV-13b, the creep strength of the various fill materials can be estimated as a function of time. Design values for short-term (24 hours) and long-term (25 years) creep strength are presented in Table IV-8.

b. Elastic Properties of Bonded Fill Materials

Elastic moduli for frozen soils have been shown to be dependent on temperature and strain-rate much like that of stress or peak strength. For example, the data of Parameswaren, 1980 show the following approximate relationship between initial tangent modulus and strain rate for frozen Ottawa sand:

$$E_i = A\ (\dot{\epsilon})^m \qquad \text{(IV-22)}$$

Table IV-8. Mechanical properties of bonded fill materials

	Initial Tangent Modulus (ksf)		Poisson's Ratio	Shear Strength		One-Dimensional Compression	
	Short Term	Long Term	μ	Short Term (24 hrs.)	Long Term (25 yrs.)	m	a
Ice-Free Gravel Placed below sea level, uncompacted σ_3 = 1.34 ksf @ 20 ft.	1400	200	0.25	4.6	1.4	1500	0.90
Gravel-Ice Mixtures Placed in the dry, compacted (recrystallized) σ_3 = 0.61 ksf @ 10 ft.	3000	550	0.25	10.0	3.7	400	0.75
Placed below sea level, uncompacted σ_3 = 1.19 ksf @ 20 ft.	2850	400	0.15	9.5	2.8	625	0.90
Silty Sands - Hydraulic Fill Uncompacted σ_3 = 0.90 ksf @ 15 ft.	1850	250	0.25	6.1	1.8	125	0.75
Compacted σ_3 = 0.94 ksf @ 15 ft.	2300	350	0.30	7.6	2.3	220	0.90

Notes:

1. For average fill temperature = 5°C.
2. σ_3 assumed = 0.5 x (overburden pressure) for average depth within the fill.
3. Short-term assumed to be 24 hours; $\frac{E_i}{S_u} = 300$.
4. Long-term assumed to be 25 years; $\frac{E_i}{S_u} = 150$.
5. Properties will vary from unbonded to fully bonded depending upon degree of recrystallization.

Comparison of Equations IV-22 and IV-13 suggests that the initial tangent modulus may be estimated from the creep strength if exponents m and n are approximately equal and if temperature effects are similar. If the ratio E_i / σ_{max} is evaluated over the full range of strain rates and temperatures reported by Parameswaren, the values range from $39 \leq E_i / \sigma_{max} \leq 221$ with an average value of 133. In general, the lower values correspond to lower strain rates; however, the variations with temperature are inconclusive.

Sayles and Haines (1974) reported peak strength and tangent modulus data for Hanover silt and Suffield clay for a range of temperatures and a strain rate of about 0.15 min^{-1}. For temperatures between 31^0 and 15^0F, the ratio of modulus to strength ranged from 273 to 138 for Hanover silt and 124 to 165 for Suffield clay. The values for Hanover silt are in the same range as Parameswaren's Ottawa sand data for comparable strain rates. Temperature effects for these soils are similarly inconclusive.

Based on the data discussed above, we conclude that the initial tangent modulus for bonded fill materials can be approximated by:

$$\frac{E_i}{\frac{1}{2}\left[\sigma_1 - \sigma_3\right]_{max}} = \frac{E_i}{S_u} = \begin{cases} 300 \text{ for short-term loads} \\ 150 \text{ for long-term loads} \end{cases} \qquad \text{(IV-23)}$$

Vinson (1978) has tabulated values of Poisson's ratio for a wide variety of soil types. The reported values for sands range from 0.23 to 0.28. For silts, the range is from about 0.28 to 0.39 with an average value of about 0.30.

Recommended design values of initial tangent modulus and Poisson ratio for the various bonded fill materials are presented in Table IV-8.

c. Compressibility

Tsytovich (1975) has reported measured values of the coefficient of volume compressibility, $m_v = \frac{\epsilon_v}{\sigma_v}$, for several frozen soils. These data indicate that m_v varies with soil type, density, and unfrozen water content.

Referring to Equation IV-11, it can be seen that m_v is the inverse of the compression modulus, m, i.e.,

$$m = \frac{1}{m_v} \qquad \text{(IV-24)}$$

In Figure IV-17, Tsytovich's data for a frozen sand and a silty sand are superimposed on a plot presented by Janbu (1967), for unfrozen soils, showing the variation of compression modulus number, m, and stress exponent, a, with porosity. To make this comparison, the porosity for frozen soils is related to only that portion of the pore volume not filled with ice, i.e.,

$$n = \frac{\text{non-ice pore volume}}{\text{total volume}} \qquad \text{(IV-25)}$$

$$n = \frac{e - i(G_s/G_i)}{1+e}$$

The data for frozen sand and silty sand are quite limited and cover only a narrow range of non-ice porosity. However, these data can be extrapolated by noting that as the amount of ice in the pores decreases to zero, the curves for the frozen and unfrozen conditions must converge at the porosity of the equivalent unfrozen soil. The resulting curve defines the variation of n with non-ice porosity for the frozen soils.

To obtain similar curves for the project fill materials, a family of parallel curves was constructed, each of which merges with the curve for the unfrozen condition at the expected placement porosity. The assumption that these curves should be parallel is based on Janbu's data for unfrozen soils. Values of the stress exponent, a, are obtained using the same type assumption regarding the influence of non-ice porosity.

To illustrate the compression parameters in the frozen versus unfrozen conditions, points for each of the fill materials for both conditions are plotted on Figure IV-17. The compression parameters for bonded fill materials are also tabulated in Table IV-8.

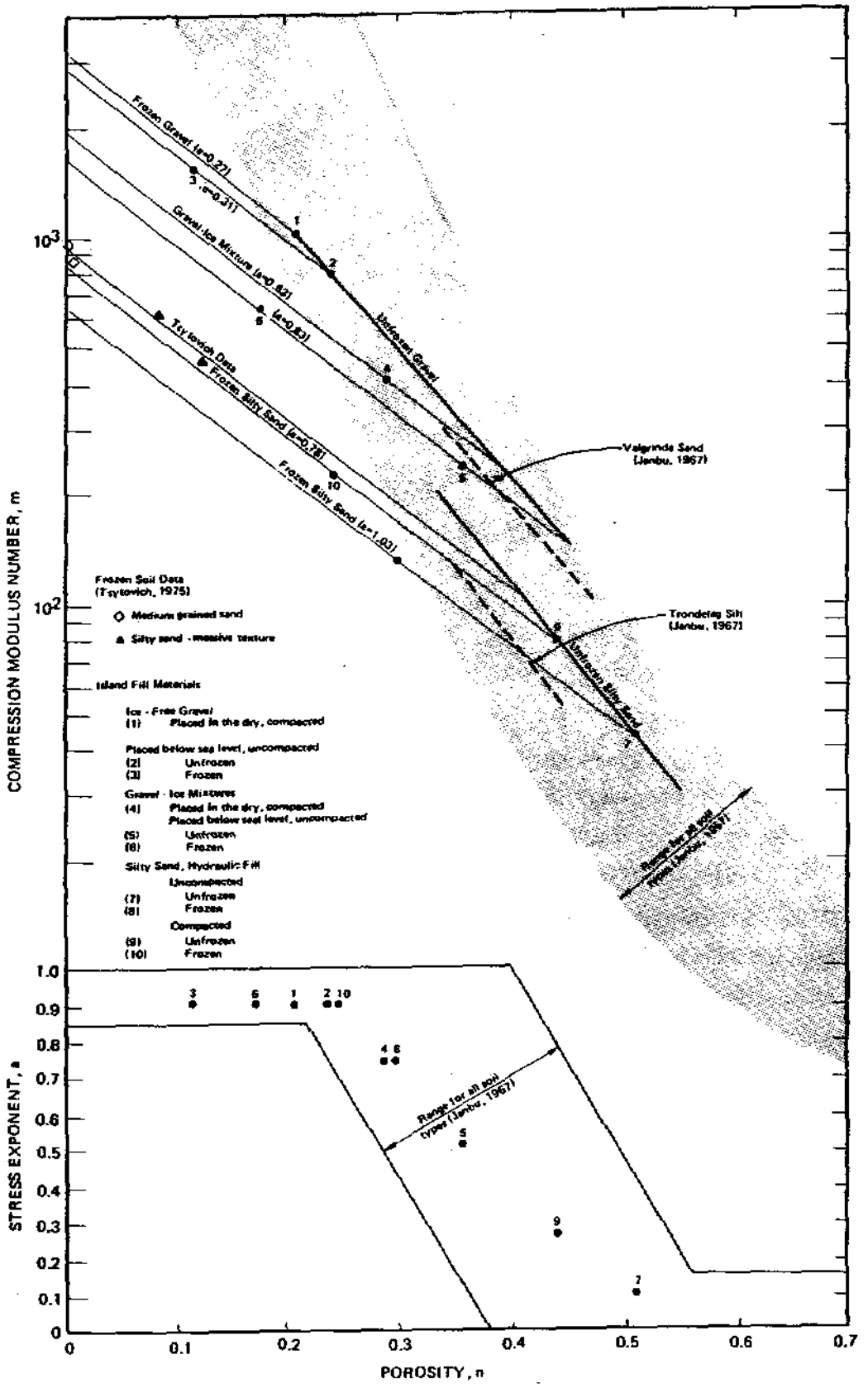

Figure IV-17. Compression parameters for island fill materials

B. PILE SETTLEMENT

As discussed in Section VII subsurface temperatures fluctuate seasonally and cause variations in pile settlement velocity. To account for this change in settlement velocity throughout the year, a representative soil temperature profile, an average for the full year, was determined. The procedure presented on Plate E-1 describes the method used to determine the "average" temperature profile for a pile embedment depth of 10 feet. This procedure was repeated for other pile embedment depths to allow development of a representative soil temperature profile. The procedure used to calculate the ground temperature profiles is presented on Plate E-2. The ice flow law presented on Plate E-3 was used to calculate pile settlement.

Procedure for determining a representative temperature profile and settlement for a 10-foot pile embedment depth.

1. The year was divided into eight time periods of equal duration as shown in Figure 1.

2. The ground temperature variation with depth was determined for each time period assuming a homogeneous soil beneath the active layer and using Equation E1 (presented on Plate E-2)for a damped, sinusoidal temperature oscillation.

3. The following was computed for the 10-foot pile embedment depth using the Ice Flow Law presented on Plate E-3.

   a. The settlement of the pile was calculated based upon an average temperature along the pile at each time period as shown in Figure 2 using Equations E2 and E3.

   δ/a = (pile settlement)/(pile diameter) Equation E2

   $\delta/a = (\dot{U}/a)\ (\Delta t) = 4.5\ (\beta ave)\ (\tau ave^n)\ (\Delta t)$ Equation E3

   where $\beta ave = f(T\ ave)$ From Figure 1, Plate E-3

   $$\frac{\delta/a}{(\tau ave^n)\ (\Delta t)} = 4.5\ (\beta ave)$$

   Note: τave^n and Δt are constant.

   b. The settlement for all time periods was added to determine the total settlement of the pile for the year using Equation E4.

   $$(\delta/a)_{ave} = \frac{\sum_{t/p=0/8}^{t/p=7/8} \frac{\delta/a}{(\tau ave^n)\ (\Delta t)}}{8}$$ Equation E4

   c. This settlement was used to compute a representative ground temperature (Trep) using Equation E5, Morgenstern's flow law, described on Plate E-3.

   $$\beta rep = \frac{\delta/a\ ave}{4.5\ (\tau ave^n)\ (\Delta t)} = 3.4 \times 10^{-6}\ psi^{-3} \times year^{-1}$$

   T rep = -4.7^{o} C From Figure 1, Plate E-3

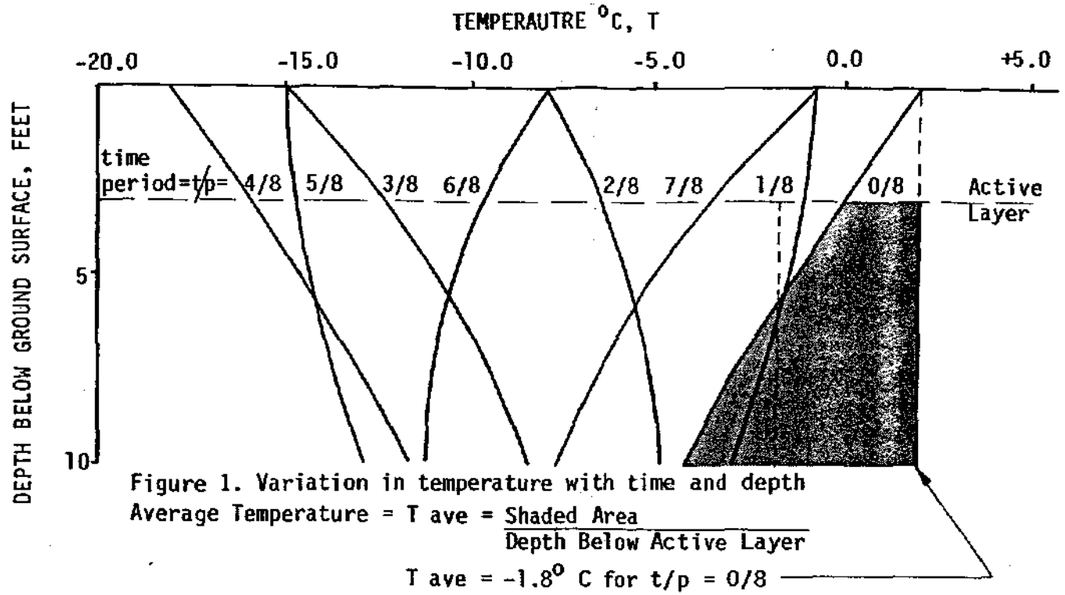

Figure 1. Variation in temperature with time and depth

Average Temperature = T ave = $\frac{\text{Shaded Area}}{\text{Depth Below Active Layer}}$

T ave = -1.8^{o} C for t/p = 0/8

t/p	0/8	1/8	2/8	3/8	4/8	5/8	6/8	7/8
T ave	-1.8^{o} C	-2.0	-5.4	-9.6	-14.2	-14.0	-10.6	-6.4
βave	8.4×10^{-6} $psi^{-3} year^{-1}$	7.6	3.0	1.7	1.2	1.2	1.6	2.6
$\frac{\delta/a}{(\tau ave^n)(\Delta t)}$	3.78×10^{-5}	3.42	1.35	0.77	0.54	0.54	0.72	1.17

Figure 2. Pile Settlement for Each Time Period

Harding Lawson Associates
Engineers, Geologists & Geophysicists

Procedure for Determining Pile Settlement and Temperature Profile
Pt. Thomson Development Project, Winter 1982
Geotechnical Study, EXXON Company, U.S.A.

PLATE E-1

DRAWN	JOB NUMBER	APPROVED	DATE	REVISED	DATE
JP	9612,031.08	DEB	4/82		

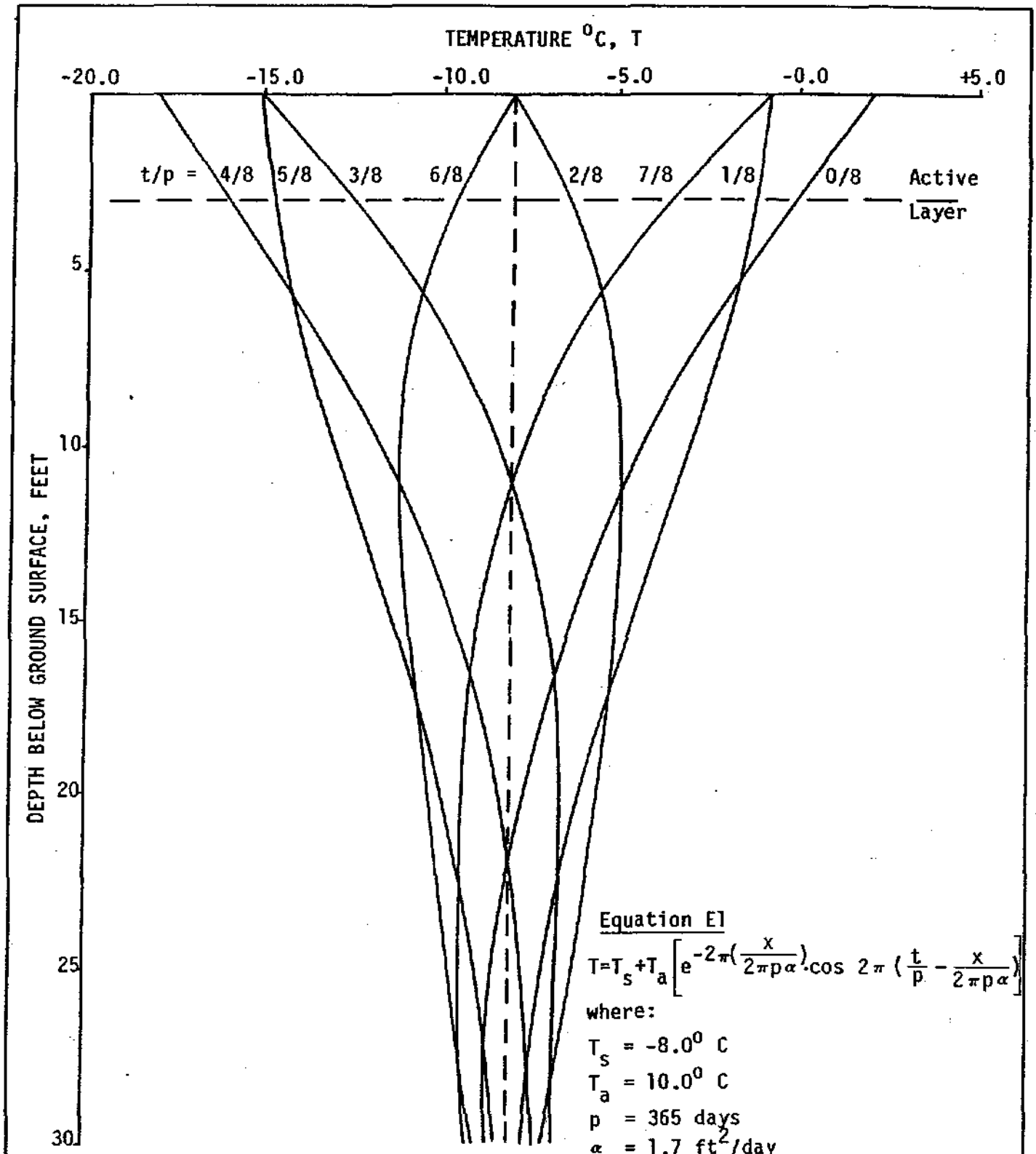

Equation E1

$$T = T_s + T_a \left[e^{-2\pi \left(\frac{x}{2\pi p \alpha} \right)} \cdot \cos 2\pi \left(\frac{t}{p} - \frac{x}{2\pi p \alpha} \right) \right]$$

where:

T_s = -8.0^0 C

T_a = 10.0^0 C

p = 365 days

α = 1.7 ft^2/day

t = time, days

x = depth below ground surface, feet

Harding Lawson Associates
Engineers, Geologists & Geophysicists

Ground Temperature Distribution
Pt. Thomson Development Project
Winter 1982, Geotechnical Study
EXXON Company, U.S.A.

PLATE **E-2**

DRAWN	JOB NUMBER	APPROVED	DATE	REVISED	DATE
JF	9612,031.08		4/82		

Ice-Flow Law (Morgenstern, Roggensack and Weaver, 1980)

$$\frac{\dot{U}_a}{a} = \frac{3^{\left(\frac{n+1}{2}\right)} \beta \tau_a^{\,n}}{n-1} = 4.5\, \beta \tau_a^{\,n} \qquad \text{Equation E5}$$

where:

U_a = pile velocity

a = pile radius

τ_a = constant tangental shear stress on ice-rich soil

n = soil creep exponent

β = soil creep constant

Temperature ^{o}C	n	K P_a^{-n} x $year^{-1}$	psi^{-3} x $year^{-1}$
-1	3	4.5×10^{-8}	1.5×10^{-5}
-2	3	2.0×10^{-8}	6.6×10^{-6}
-5	3	1.0×10^{-8}	3.3×10^{-6}
-10	3	5.6×10^{-9}	1.8×10^{-6}

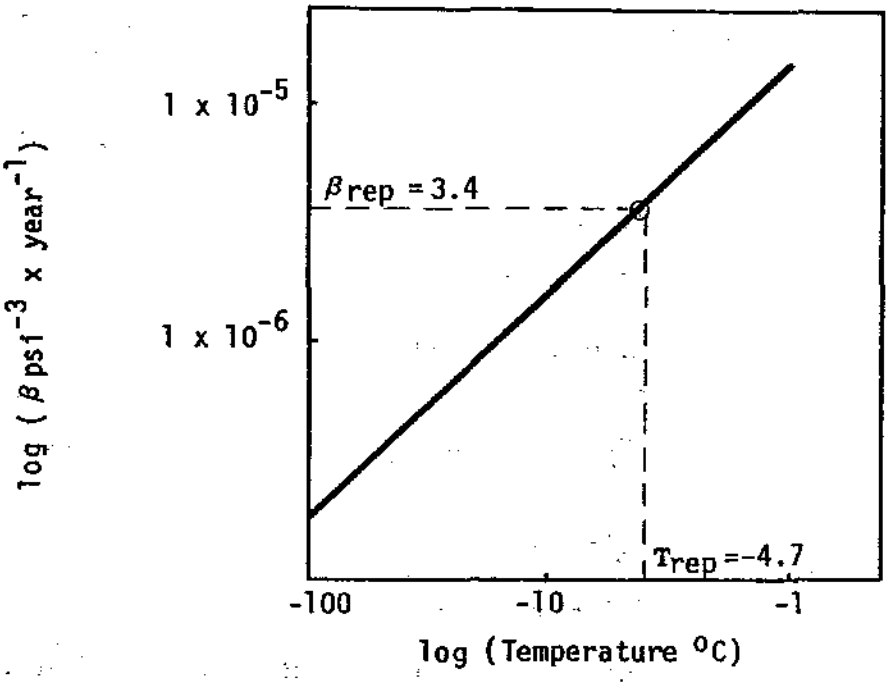

Figure 1. Temperature Vs Soil Creep Constant

Harding Lawson Associates
Engineers, Geologists & Geophysicists

Ice Flow Law
Pt. Thomson Development Project
Winter 1982, Geotechnical Study
EXXON Company, U.S.A.

PLATE **E-3**

DRAWN	JOB NUMBER	APPROVED	DATE	REVISED	DATE
JP	9612,031.08		4/82		

C. ANALYSIS OF LATERALLY LOADED PILES

ANALYSIS OF LATERALLY LOADED PILES IN PERMAFROST

The behavior of piles subjected to lateral loading may be analyzed by the subgrade-reaction method (Poulos and Davis, 1980). The method is capable of treating non-linear soil behavior, layered soils and non-uniform pile sections, and is readily adaptable to computer solution. In general, the soil response to lateral loads is modeled as a series of unconnected non-linear springs represented by "P-Y curves". The P-Y curves are a representation of the load-deflection characteristics of the soil at a given depth along the pile and depend upon the pile dimesions as well as the stress-strain and strength characteristics of the soil.

P-Y Curves

Procedures for constructing the P-Y curves for various (unfrozen) soil types and loading conditions have been summarized by Reese (1975). An example of these procedures (for soft, saturated clays) is as follows:

1. The ultimate soil resistances per unit length of pile shaft, P_{ult}, is computed using:

$$P_{ult} = N_p \cdot c_f \cdot d \qquad (1)$$

where c_f = shear strength

d = pile diameter or width

N_p = nondimensional ultimate resistance coefficient

N_p increases from a value of 3 at ground surface to a maximum value of 9 at a depth of several pile diameters; vis.,

$$N_p = 3 + \frac{\sigma_v}{c_r} + J \cdot \frac{x}{d} \quad (2)$$

where σ_v = overburden pressure at depth x

x = depth

J = empirical coefficient (typically, J = 0.5)

2. The P-Y curve is approximately by a cubic parabola:

$$P = 1/2\ P_{ult} \left(\frac{Y}{Y_c} \right)^{1/3} \quad (3)$$

where P = soil reaction for lateral pile deflection, y

Y_c = lateral pile deflection at which $P = 1/2\ P_{ult}$

Note: This procedure is based on the concept that the stress-strain curve for the soil and the P-Y curve for soil reaction on the pile should have similar shapes as illustrated in Figure 1 (Matlock, 1970).

3. Y_c is approximated by:

$$Y_c = 2.5\ \epsilon_c \cdot d \quad (4)$$

where ϵ_c = strain at which $(\sigma_1 - \sigma_3) = 1/2\ (\sigma_1 - \sigma_3)_{ult}$

Stress-Strain-Time Behavior of Frozen Soils

The stress-strain behavior of frozen soil depends upon, among other factors, the duration of loading and the soil temperature. For example, when a sample of frozen soil is subjected to a constant uniaxial stress, the sample continues to deform with time. As shown on Figure 2 a typical strain-time (creep) curve for frozen soil may exhibit three stages: (1)

deccelerating, or primary, creep; (2) constant strain-rate, or secondary creep; and (3) accelerating, or tertiary, creep which usually leads rapidly to failure.

Depending upon the type of frozen soil and the applied stress level, any of the three stages of creep may dominate (Figure 2a).

Ladanyi (1978) has suggested that primary creep of frozen soils can be described by the equation:

$$\dot{\epsilon} = b\left(\frac{\dot{\epsilon}_c}{b}\right)^{b}\left(\frac{\sigma_1-\sigma_3}{\sigma_c}\right)^{n} \cdot t^{(b-1)} \qquad (5)$$

in which $\dot{\epsilon} = d\epsilon/dt$ = strain-rate

$(\sigma_1-\sigma_3)$ = applied principle stress difference

t = elapsed time

σ_c $\dot{\epsilon}_c$ = values of $(\sigma_1-\sigma_3)$ and $\dot{\epsilon}$ at an arbitrarily selected time

n = stress exponent

b = time exponent

σ_c, $\dot{\epsilon}_c$, n, b = temperature-dependent material constants

Equation (5) predicts that, in the primary creep stage, a plot of log ($\dot{\epsilon}$) vs. log (t) will be linear with a slope equal to (b-1).

In secondary creep, the strain-rate is independent of time (b=1 in Equation 5), so that:

$$\dot{\epsilon} = \dot{\epsilon}_c\left(\frac{\sigma_1-\sigma_3}{\sigma_c}\right)^{n} \quad \{\text{secondary creep}\} \qquad (6)$$

Equations 5 and 6 both predict that a plot of log ($\dot{\epsilon}$) vs. log (σ_1-σ_3) will be linear with a slope equal to n. However, the value of the stress exponent, n, may be significantly different in the primary and secondary stages.

The constants in Equations 5 and 6 are temperature-dependent. The temperature effects may be evaluated by performing creep tests at different temperatures or estimated from published data.

Evaluation of Creep Parameters of Design

At the stress levels and load durations normally used in engineering design, it is often assumed that secondary creep dominates (Ladanyi, 1978). However, test durations of two weeks or more may be required to establish secondary creep rates at design stress levels. An alternative approach is to perform relatively short-term (a few hours) creep tests and extrapolate the primary creep behavior to the onset of secondary creep (Figure 3). This requires an estimate of the time at which the transition from primary to secondary creep will occur. If the time for this transition to occur is underestimated, the extrapolated secondary creep rate will be conservative (too fast) and, if overestimated, the secondary creep rate will be unconservative (too slow).

Figure 4 shows the primary creep behavior of a sample which was step-loaded to three different stress levels. Except for the usual experimental data scatter, the log ($\dot{\epsilon}$) vs. log (t) relationship appears to be linear as predicted by Equation 5. On the other hand, contrary to Equation 5, the curves are not parallel; i.e., n $\neq$ constant. These

diverging curves suggest that n steadily increases through the primary stage to the onset of secondary creep. Thus, the steady-state n value obtained by extrapolation will be dependent upon the time estimated for the onset of secondary creep. In this context, as noted previously, underestimating the transition time from primary to secondary creep will be conservative.

For our laboratory test data, we have estimated the time to onset of secondary creep to be 24 hours. We believe this to be a conservative choice. The extrapolated 24-hour strain rates for several tests at different temperatures are plotted vs. the applied stress on a log-log scale in Figure 5. The slope of the straight lines fitted through the data points for each temperature is equal to the stress exponent, n, in Equation 6. For these data n = 3, which is consistent with published data on ice-rich soils (Morgenstern et.al, 1980). The values of $\dot{\epsilon}_c$ and σ_c can also be obtained fromm any convenient point on each line e.g., for 28^0F, we could choose, say $\dot{\epsilon}_c = 10^{-6}$ min^{-1} and σ_c = 20 psi.

The effect of temperature can also be deduced from Figure 5. For example, at $\dot{\epsilon} = 2 \times 10^{-4}$ min^{-1}, the corresponding stress values at 28^0, 25^0, and 20^0 are 55 psi, 78 psi and 150 psi respectively. As shown on Figure 6, the relationship between stress and temperature (for a given strain-rate) is essentially linear.

Equation 6 and the laboratory creep test results (examples of which are presented on Figures 4, 5, and 6) form the basis for establishing the P-Y curves for the ice-rich fine-grained permafrost in the upper 7.5 feet of the subsurface profile. The fact that the stress exponent, n, is equal to 3.0 for the laboratory test data is consistent with the use of a cubic parabola to represent the P-Y curves since Equation 6 can be rewritten in the form:

$$\sigma_1 - \sigma_3 = \sigma_c \left(\frac{\epsilon}{\dot{\epsilon}_c \cdot t} \right)^{1/n} \tag{7}$$

in which t = any elapsed time (short of failure). In this application "t" is the duration of loading for the various loading conditions.

To construct the P-Y curves, the soil creep parameters required are the creep shear strength (Equation 1) and the strain corresponding to half of the ultimate creep strength (Equation 4). For a given duration of loading and soil temperature, Equation 7 can be solved for:

$$(\sigma_1 - \sigma_3)_f = 2 c_f = \sigma_c \left(\frac{\epsilon_f}{\dot{\epsilon}_c \cdot t_d} \right)^{1/n} \tag{8}$$

in which c_f = $1/2\ (\sigma_1 - \sigma_3)_f$ = creep shear strength

ϵ_f = strain at which the soil fails in creep

t_d = load duration for a particular design condition

Also, for n = 3,

$$\epsilon_c = 1/8 \cdot \epsilon_f \tag{9}$$

Consider the following example:

1. Assume $T = 28^{o}F$
   $\epsilon_f = 0.2$
   $t_d = 24$ hours

2. From Figure 5, say $\dot{\epsilon} = 2 \times 10^{-4}$ min^{-1}
   $\sigma_c = 55$ psi

3. From Equation 8, $c_f = \left(55 \times \frac{0.2}{2 \times 10^{-4} \times 24 \times 60}\right)^{1/3} = 24.4$ psi

*** The following steps depend upon pile diameter and depth***

4. Substitue c_f into Equations 1 and 2 to obtain P_{ult}

5. From Equation 9, $\epsilon_c = 0.025$
   Substitute ϵ_c into Equation 4 to obtain Y_c

6. Construct the P-Y curve using Equation 3

The foregoing procedure was developed specifically for ice-rich fine-grained soils for which laboratory creep data was available. Basically the same procedure was used to develop the P-Y curves for the underlying ice-poor granular soils except that the creep parameters were estimated from published data (Sayles, 1968) due to the lack of suitable samples for laboratory testing. As can be inferred from the P_{ult} - Y_c data previously supplied, the ice-poor soils have greater creep strengths and fail at lower strains than the ice-rich soils. Also, the stress exponent, n, was estimated to be 7.5 for the ice-poor soils.

Frozen soils tend to go from ductile behavior at low strain-rates to brittle behavior at high strain-rates. Therefore, ϵ_c for three-minute loadings were taken to be one-half the values used for 24-hour and 20-year loadings.

REFERENCES

Ladanyi, B. 1978. "Mechanical Properties of Frozen Ground," Geotechnical Engineering for Cold Regions. (Andersland and Anderson, eds.), McGraw-Hill Book Company.

Matlock, H. 1970. "Correlations for Design of Laterally Loaded Piles in Soft Clay." Proc. 2nd Offshore Tech. Conf., Houston, vol. I: 577-594.

Morgenstern, N. R., et.al. 1980. "The Behavior of Friction Piles in Ice and Ice-Rich Soils," Canadian Geotechnical Journal, vol. 17, pp. 405-415.

Poulos, H. G. and Davis, E. H. 1980. Pile Foundation Analysis and Design, John Wiley and Sons.

Reese, L. C. 1975. "Laterally Loaded Piles." Proc. of the Seminar Series, Design, Construction and Performance of Deep Foundations; Geot. Group and Continuing Education Committee, San Francisco section, ASCE; Univ. of Calif., Berkeley.

Sayles, F. H. 1968. "Creep of Frozen Sands", U.S. Army Cold Reg. Res. Engl. Lab (CRREL), Report 190, Hanover, N.H.

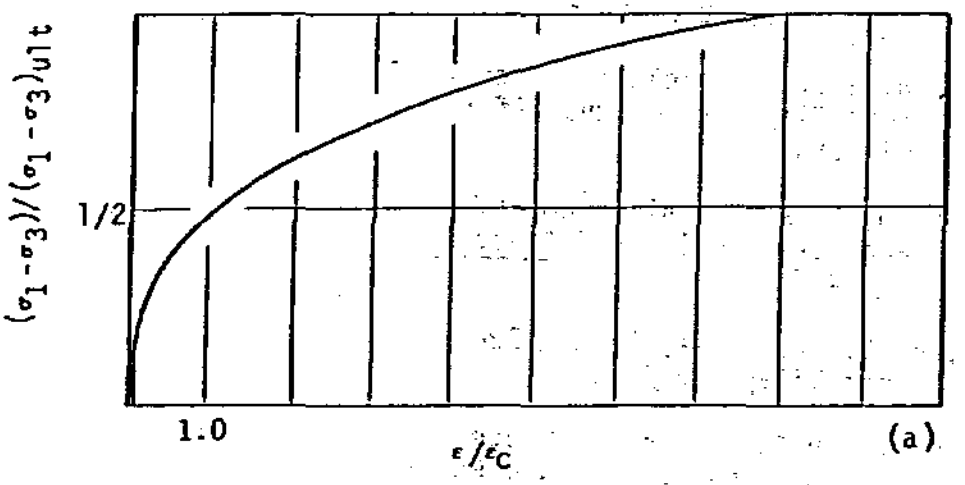

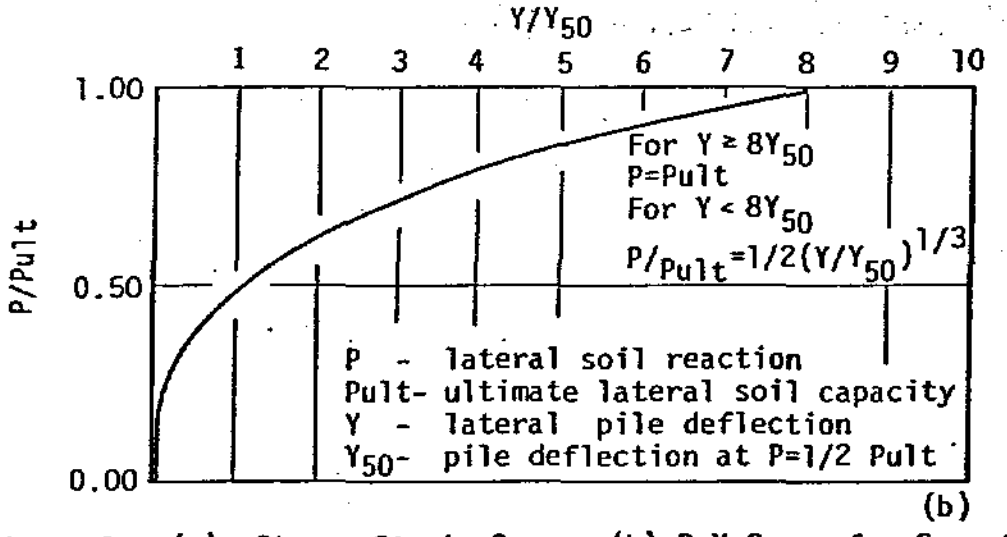

Figure 1. (a) Stress-Strain Curve, (b) P-Y Curve for Same Soil

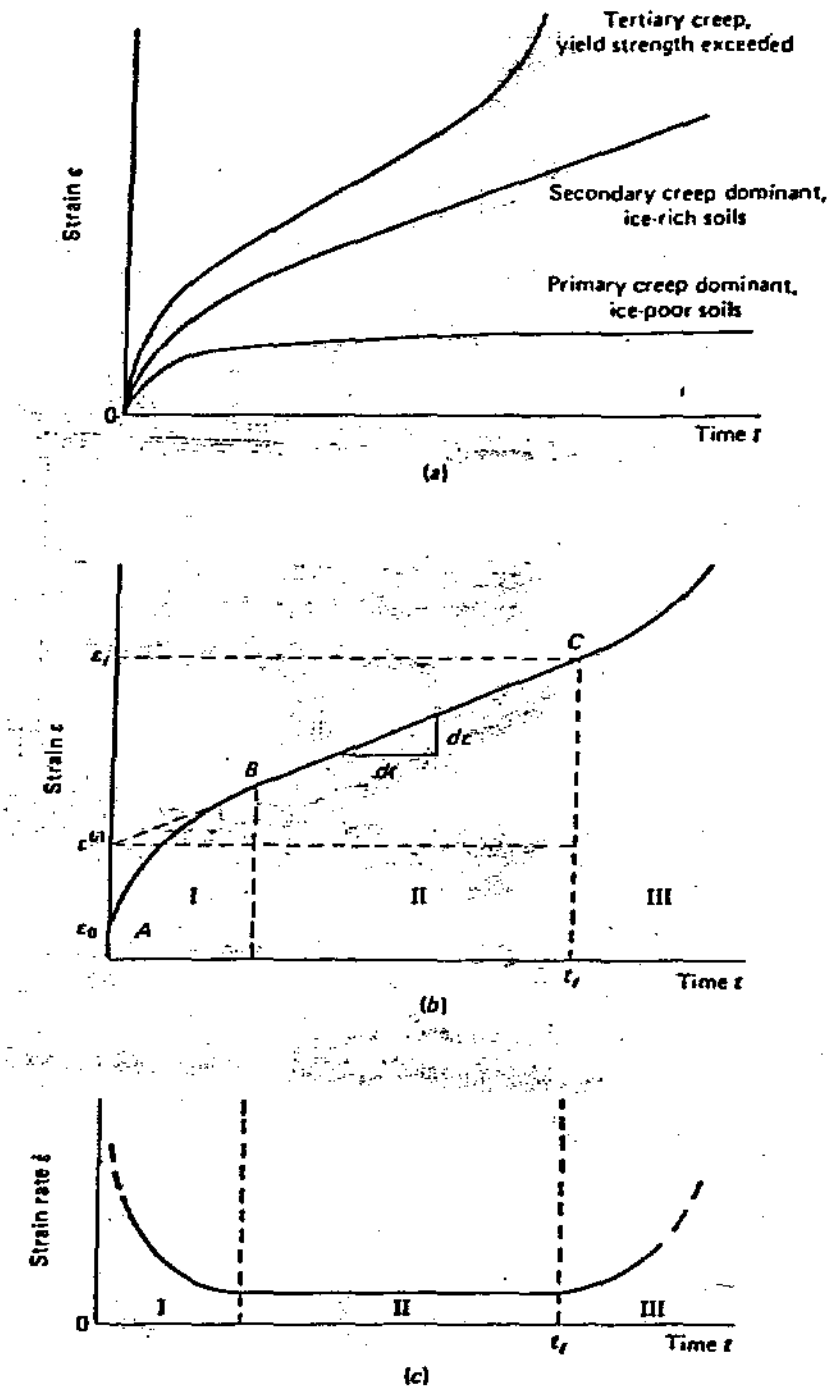

Figure 2. Constant-stress creep test: (a) creep-curve variations; (b) basic creep curve; (c) true strain rate vs. time. (after Ladanyi, 1978)

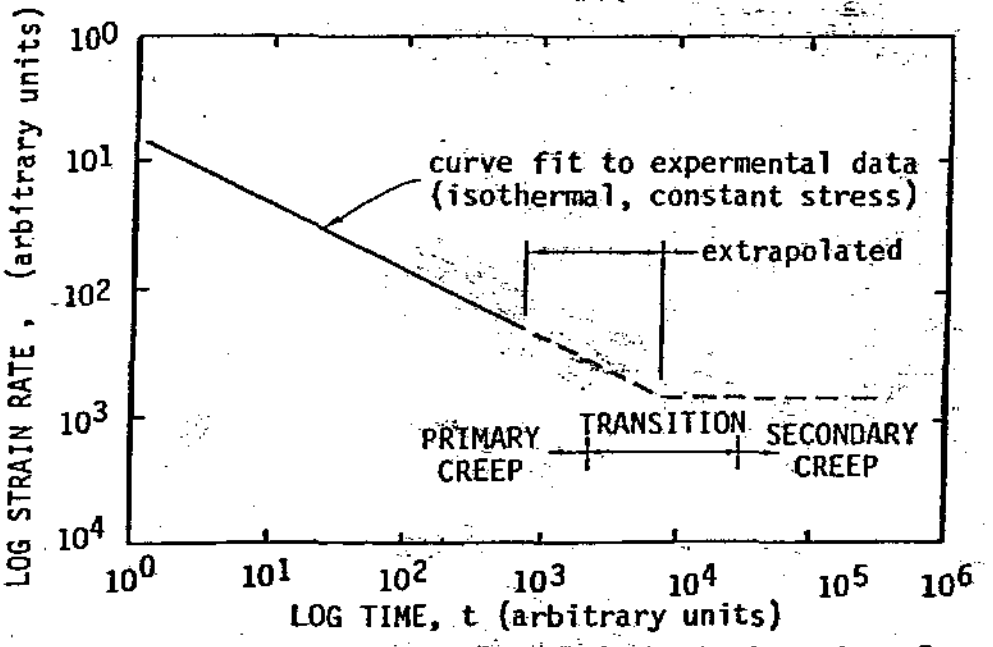

Figure 3. Extrapolation from Primary to Secondary Creep

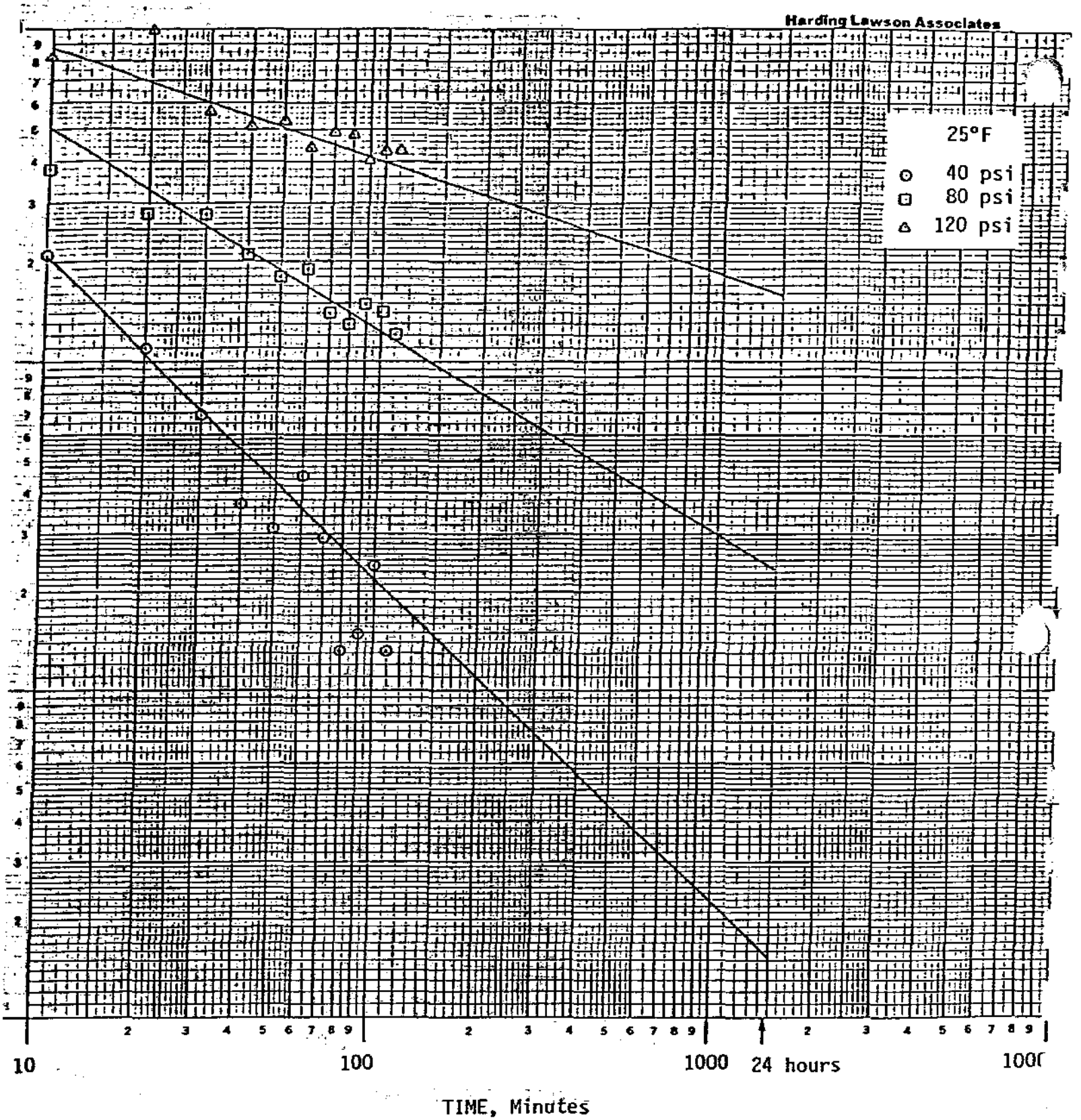

Figure 4. Primary creep behavior : Ice-Rich Soils

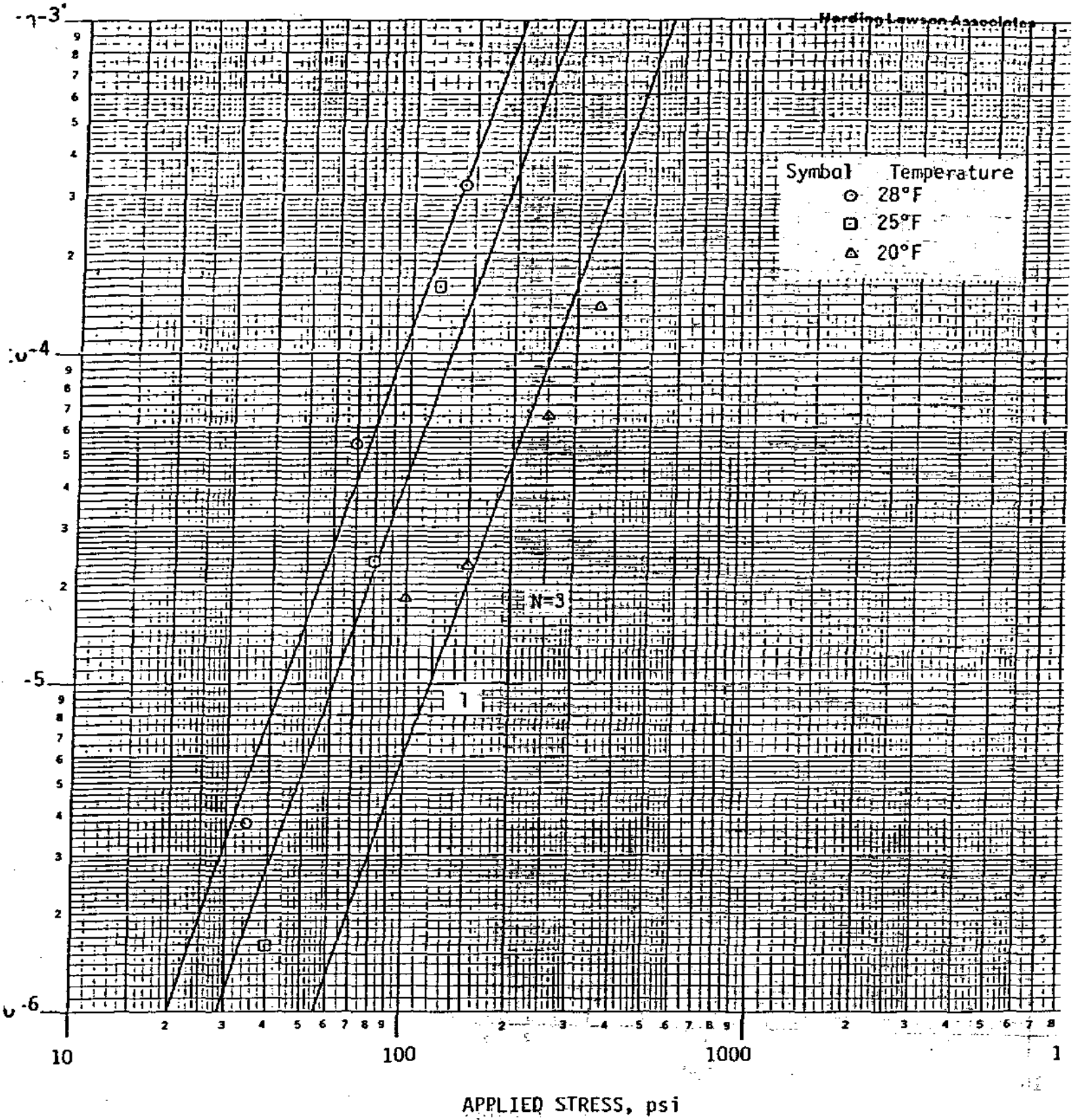

Figure 5. Secondary creep rates at 24 hours (extrapolated from primary creep data)

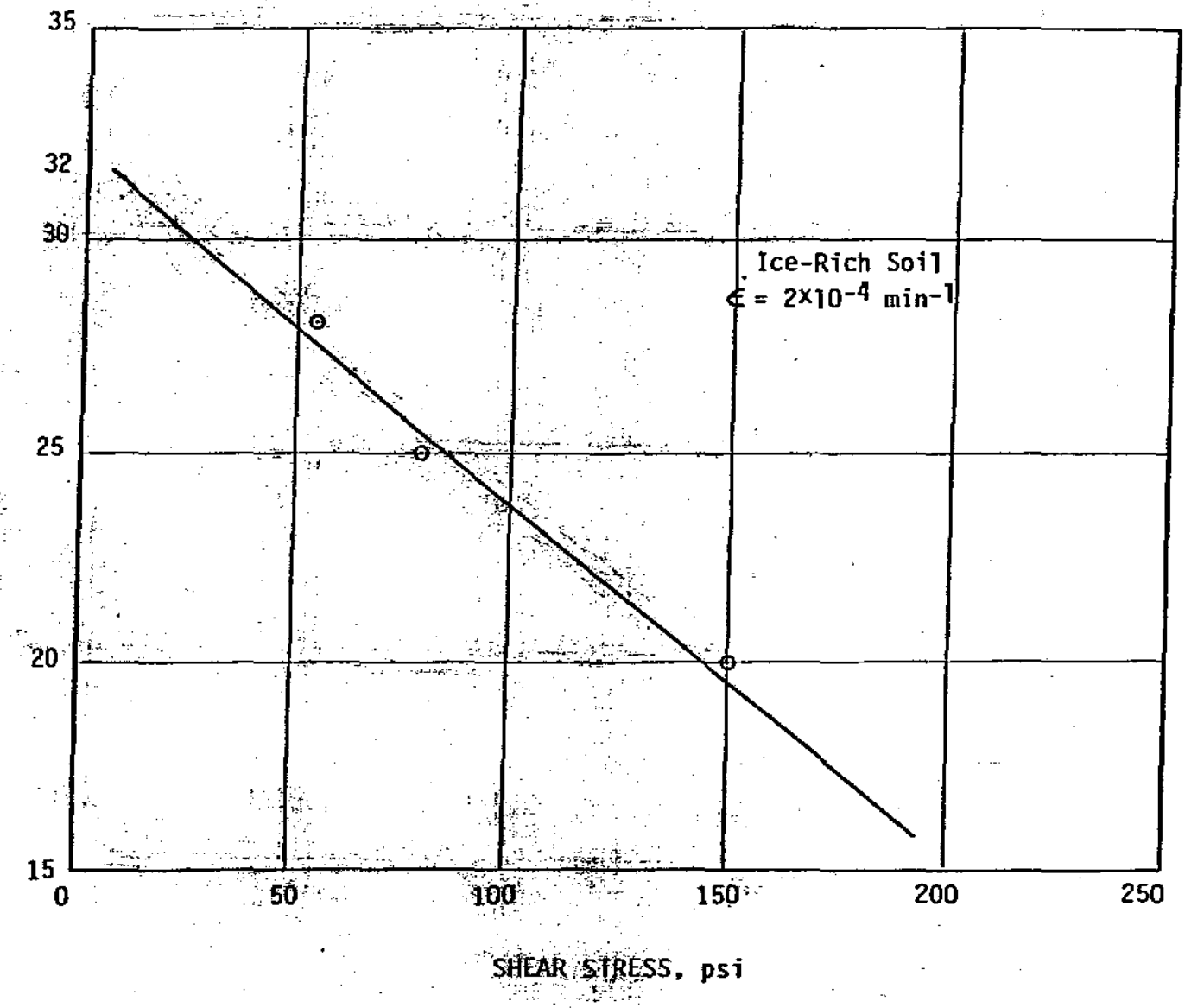

Figure 6. Effect of temperature on creep of Ice-Rich Soils